Food & Function

ROYAL SOCIETY OF CHEMISTRY

PAPER

Cite this: *Food Funct.*, 2021, **12**, 892

Berbamine induced activation of the SIRT1/LKB1/AMPK signaling axis attenuates the development of hepatic steatosis in high-fat diet-induced NAFLD rats

Ankita Sharma,[a,b] Sumit Kr Anand,[a,c] Neha Singh,[a,c] Akshay Dwarkanath,[a] Upendra Nath Dwivedi[b] and Poonam Kakkar *[a,c]

Non-alcoholic fatty liver disease (NAFLD), a chronic metabolic disorder is concomitant with oxidative stress and inflammation. This study aimed to assess the effects of berbamine (BBM), a natural bisbenzyl-isoquinoline alkaloid with manifold biological activities and pharmacological effects on lipid, cholesterol and glucose metabolism in a rat model of NAFLD, and to explicate the potential mechanisms underlying its activity. BBM administration alleviated the increase in the body weight and liver index of HFD rats. The aberrations in liver function, serum parameters, and microscopic changes in the liver structure of HFD fed rats were significantly improved upon BBM administration. BBM also significantly attenuated oxidative damage and inhibited triglyceride and cholesterol synthesis. The SIRT1 deacetylase activity was also enhanced by BBM through liver kinase B1 and activated AMP-activated protein kinase. Activation of the SIRT1/LKB1/AMPK pathway prevented the downstream target ACC (acetyl-CoA carboxylase) and elevation in the expression of FAS (fatty acid synthase) and SCD1 (steroyl CoA desaturase). BBM also modulated the expression of PPARs maintaining the fatty acid homeostasis regulation. The assessment of berbamine induced ultrastructural changes by TEM analysis and the expression of autophagic markers LC3a/b, Beclin 1 and p62 revealed the induction of autophagy to alleviate fatty liver conditions. These results show novel findings that BBM induced protection against hepatic lipid metabolic disorders is achieved by regulating the SIRT1/LKB1/AMPK pathway, and thus it emerges as an effective phyoconstituent for the management of NAFLD.

Received 22nd September 2020,
Accepted 9th December 2020

DOI: 10.1039/d0fo02501a

rsc.li/food-function

1. Introduction

Non-alcoholic fatty liver disease (NAFLD) is a manifestation of metabolic syndromes characterized histologically by steatosis which may eventually progress to serious conditions including steatohepatitis, fibrosis, irreversible cirrhosis, and hepatocellular carcinoma.[1] NAFLD is emanating as a risk factor for diabetes and cardiovascular disease making it a major public-health trepidation in the world since it affects more than 40% of the population in some countries.[2] The pathogenesis of NAFLD is a multifarious process abetted by lipid metabolism disorders, chronic inflammation, and oxidative stress.[3] The pathological features of NAFLD were earlier explained using a 'two-hit' model wherein the first hit is insulin resistance induced lipid accumulation in hepatocytes and the second hit is due to oxidative stress, mitochondrial dysfunction and lipid peroxidation mediated inflammation.[4] Additionally, the 'third hit' is also being taken into consideration, which is due to mature hepatocytes not being replicated because of culpability in regeneration processes.[5]

AMPK, the AMP-responsive kinase, is a central metabolic switch found in all eukaryotes that is activated by cellular energy deprivation as reflected by an increased AMP/ATP ratio. AMPK activation is also mediated by the upstream kinases LKB1 (the tumor suppressor kinase), and CaMKKβ (Ca^{2+}/calmodulin-dependent protein kinase kinase-β).[6] Upon activation, it initiates several metabolic and genetic events to restore the ATP levels. AMPK stimulates ATP generation processes such as fatty acid oxidation whereas subdues non-critical ATP consuming processes such as triglyceride and protein synthesis.[7] AMPK activation also increases mitochondrial carbohydrate and lipid oxidation to increase ATP production *via* the Krebs cycle and oxidative phosphorylation. SIRT1 (sirtuin 1), a NAD-dependent sirtuin class of histone/protein,

[a]*Herbal Research Laboratory, CSIR-Indian Institute of Toxicology Research (CSIR-IITR), Vishvigyan Bhawan, 31, Post Box No. 80, Mahatma Gandhi Marg, Lucknow-226001, India. E-mail: kakkarp59@gmail.com; Tel: +91 9335902630*
[b]*Department of Biochemistry, University of Lucknow, Lucknow, 226007, India*
[c]*Academy of Scientific and Innovative Research (AcSIR), Ghaziabad-201002, India*

plays an imperative function in cellular metabolism and stress responses by modulating the activity of various key transcription factors working in co-operation with AMPK.[8] SIRT1 and its activators play a quintessential role in maintaining the lipid and glucose homeostasis and also insulin sensitivity mediated *via* regulation of mitochondrial biogenesis and β-oxidation and improvement of anti-inflammatory activities.[9] Under metabolic dysregulation conditions of hyperglycemia, high-fat diet and obesity both AMPK and SIRT1 levels are downregulated in the liver.[10,11] Activation of SIRT1/AMPK signaling augments fatty-acid oxidation and limits *de novo* fatty-acid synthesis principally through deacetylation and/or phosphorylation of transcription factors or coactivators, such as forkhead box O (FoxO), peroxisome proliferator-activated receptor-γ coactivator 1α (PGC-1α) and sterol regulatory element binding protein 1 (SREBP-1).[12]

Sterol response element-binding proteins belong to the basic helix-loop-helix leucine zipper family of DNA binding transcription factors.[13] Upregulation of the SREBP-1/2 pathway in obesity and metabolic syndrome is the imperious cause of the development of NAFLD.[14,15] SREBP-1a and -1c (sterol response element-binding protein 1a and 1c, respectively) are the products of the same gene while SREBP-2 is encoded by a separate gene. SREBP-1a and -1c regulate the expression of fatty acid and triglyceride synthesis whereas SREBP-2 regulates cholesterol synthesis.[16] In response to feeding, nuclear translocation of SREBP-1c increases, and it eventually binds to its lipogenic target genes, such as fatty acid synthase, and also to its own gene, thereby stimulating hepatic lipogenesis.[17]

In addition, autophagy is an intracellular self-digestion process that plays a pivotal role in maintaining cellular homeostasis in eukaryotes by degrading old, unfolded, or damaged organelles and proteins and critically regulates hepatic lipid metabolism.[18] Previous data have shown that SIRT1-mediated autophagy induction occurs both *in vitro* in human cells and *in vivo* in Caenorhabditis elegans,[19] but the function of SIRT1 in the regulation of autophagy in the hepatic tissue of NAFLD rats is nevertheless indeterminate.

Presently, NAFLD treatments encompass a balanced diet, exercise, and drugs, including metformin, statins, and fibrates. However, there is no accord on effective drug therapy because these drugs have some contra-indications leading to the judicious use of medications. Therefore, new entrants with high competence and little or no side effects are urgently needed for the treatment of NAFLD. Presently, copious studies are focusing on herbal extracts or natural products, and various herbal products with anti-hyperlipidemic and hepatoprotective effects for the management of NAFLD.[20] Thus, it is equitable to develop effective natural products for the treatment of NAFLD. Berbamine (BBM), a bisbenzylisoquinoline alkaloid, is the major bioactive component of *Berberis amurensis.*[21] BBM possesses multiple bioactivities including anti-hypertensive, anti-arrhythmic, and anti-inflammatory, cardioprotective and immunomodulatory effects.[22,23] The antitumor activity of BBM is given high attention in recent years particularly for chronic myeloid leukemia,[24,25] breast cancer[26] and melanoma.[27] However, the metabolism and toxicity of this alkaloid have not been well investigated. Given that scarce knowledge is currently available regarding how berbamine impacts lipid metabolism and autophagy in the liver, the effects of berbamine on the autophagic mechanism of hepatic lipid will be of interest. In this study, we intended to study the potential mechanism through which berbamine mitigates the NAFLD conditions and the concomitant hepatic steatosis in a rat model of NAFLD.

2. Materials and methods

2.1 Chemicals

Berbamine dihydrochloride (Cat no. 547190) and fenofibrate (Cat no. F6020) were procured from Sigma Aldrich (St Louis, MO, United States). Cholesterol and lard were purchased from MP Biomedicals. Antibodies specific for fatty acid synthase (FAS), acetyl CoA carboxylase (ACC), phospho-ACC, steorylcoA desaturase (SCD1), CD36, AMPK, P-AMPK, mTOR, P-mTOR (Ser2448), SIRT1, LKB1, P-LKB1, LC3A/B, Beclin 1, p62, acetyllysine and horseradish peroxidase conjugated anti-goat, anti-rabbit and anti-mouse antibodies and Alexa Fluor-555 conjugated anti-rabbit and FITC conjugated anti-rabbit immunoglobulin were procured from Cell Signaling Technology (CST, Danvers, MA, USA). Monoclonal antibody for β-actin, HO-1, SOD2, and protein A/GPLUS sepharose beads (sc-2003) were purchased from Santa Cruz Biotechnology (Santa Cruz, CA). All reagents used in the study were of highest purity grade procured from Sigma-Aldrich unless otherwise stated.

2.2 Ethics statement

All methods of this study were carried out in accordance with the international guidelines and protocols and all experimental protocols were approved by the Animal Ethics Committee of CSIR-IITR (approval number IITR/IAEC/03/2018).

2.3 Animal and experimental protocols

Thirty-six male Wistar rats weighing 80–100 g were procured from the IITR animal house. All rats were housed in cages under standard conditions of controlled temperature (21–23 °C), humidity and regular light cycles (12 h). All rats had free access to water and diets corresponding to their assigned treatment group. The rats were randomly assigned to the following six groups (6 in each group, $n = 6$) as shown in Scheme 1.

Group 1: Normal control (control)

Group 2: Control group treated with BBM (150 mg per kg body weight) (H-BBM)

Group 3: HFD group (HFD)

Group 4: HFD administered with fenofibrate (100 mg per kg body weight) (HFD-FF)

Group 5: HFD administered with low-BBM (50 mg per kg body weight) (HFD-LBBM)

Group 6: HFD administered with high BBM (150 mg per kg body weight) (HFD-HBBM)

Group 1 and group 2 rats were fed a standard diet, and groups 3–6 received a high fat diet (HFD). The HFD consisted

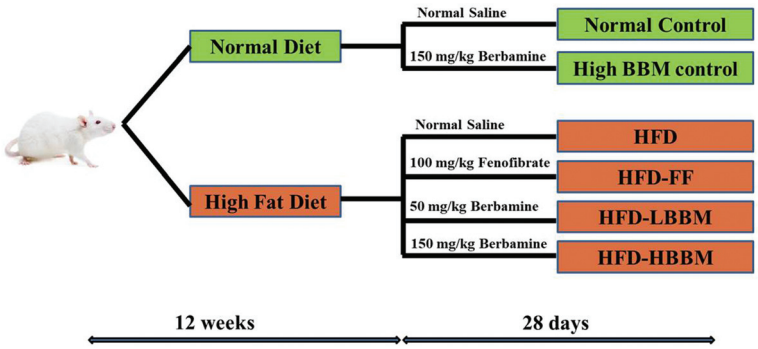

Scheme 1 Schematic diagram of experimental protocol.

Table 1 Metabolized energy

	Control diet		High fat diet	
Contents	Energy (kcal/100 g)	% metabolized energy	Energy (kcal/100 g)	% metabolized energy
Fat	36.7	11.37	185.49	40.75
Protein	76.8	23.80	66.64	14.64
Carbohydrate	209.1	64.81	202.96	44.59

of standard chow plus 2% cholesterol and 15% lard. The metabolized energy values of the standard normal diet and high-fat diet are listed in Table 1. Twelve weeks later, the rats were gavaged with BBM (groups 2, 5 and 6) dissolved in distilled water or fenofibrate (group 4) dissolved in corn oil for 28 days. The doses were selected based on previous reports and *in vitro* studies by our research group,[28] BBM was orally administered at doses of 50 and 150 mg per kg body weight.[29] Fenofibrate, a lipid regulating agent, was used as the positive control drug in this study for NAFLD.[30,31] Fenofibrate was orally administered in rats at a dose of 100 mg per kg body weight. Food intake was examined weekly and the body weight was measured twice a week during the course of the experiment.

2.4 Sample preparation

Following the experimental duration (12 weeks + 28 days), the animals were fasted overnight. The experimental animals were sacrificed by intraperitoneally injecting ketamine (100 mg per kg body weight) and their blood was collected through the inferior vena cava. Their livers were excised, weighed and sliced into three sections. The first section was secured for histological examination. The remaining two sections were snap-frozen in liquid nitrogen and preserved at −80 °C until utilized for further analysis. The visceral and epididymal fat pads were removed and weighed. For serum preparation, blood was kept in tubes that were held in a slanting position and the blood was allowed to clot for 30 minutes at room temperature, followed by centrifugation at 1000*g* for 10 minutes. The separated serum was then transferred to a clean tube and used for further analysis.

2.5 Serum biochemical analysis

The serum levels of glucose, triglycerides (TG), total cholesterol (TC), albumin, globulin, total proteins, alkaline phosphatase (ALP), aspartate aminotransferase (AST) and alanine aminotransferase (ALT) were determined with a clinical autoanalyzer (RANDOX Laboratories Limited, UK) using the kits provided by the manufacturers. For this 100 μl of serum samples were loaded into the auto-sampler and the parameters to be assessed were set. The results were expressed in mg dL^{-1} for glucose, mg dL^{-1} for triglycerides, mg dL^{-1} for cholesterol, g dL^{-1} for albumin, mg dL^{-1} for globulin, g dL^{-1} for total proteins, and U dL^{-1} for alkaline phosphatase (ALP), aspartate aminotransferase (AST) and alanine aminotransferase (ALT).

2.6 Hepatic lipid analysis

For quantitative assessment of the hepatic lipid levels, the hepatic lipids were extracted by using the method described by Folch *et al.*[32] with slight modifications. Briefly, the hepatic tissue was weighed and homogenized with 20× volume of chloroform/methanol (2 : 1) mixture. The homogenate was then subjected to vibration for 15–20 min, and the precipitate was separated by centrifugation at 2000*g* for 10 min. 0.2-fold volume of water was then added, followed by centrifugation at 2000*g* for 10 min. The lower chloroform phase was moved to a new tube and was vacuum dried. Thereafter, the lipid samples were accurately weighed and their weights were recorded.

The hepatic glycogen content was measured by the anthrone–sulfuric acid method. For this, 1 g of frozen hepatic tissue was mixed with 30% KOH for 20 min at 100 °C, and then diluted with chilled water. The resultant KOH digest was mixed gradually with the anthrone reagent (1 : 2, vol/vol) and boiled for 10 min for color development. The absorbance was read spectrophotometrically at 620 nm within 2 h (Ultrospec 3100 pro, UV visible spectrophotometer).

2.7 Histopathology

Formalin-fixed liver tissue samples were embedded in paraffin and 5 μm sections were obtained using a rotary microtome (Leica RM 2155, Germany). The sections were mounted on glass slides and stained with H&E after dehydration.

2.8 Oxidative stress and lipid peroxidation determination

For assessment of the oxidative stress and lipid peroxidation levels, frozen hepatic tissues were thawed and homogenized quickly in chilled PBS with 5 mM β-hydroxytoluene (BHT) at 10 : 1 dilution. The supernatant obtained after the centrifugation of the homogenate at 800*g* for 5 min at 4 °C was used for the biochemical determination. Lipid peroxidation in the liver homogenates and in serum was measured spectrophotometrically by the thiobarbituric acid (TBA) reaction according to the method described by Wallin *et al.*[33] Malondialdehyde (MDA), an indicator of lipid peroxidation and one of the major breakdown products of polyunsaturated phospholipids present in the cell membrane, was estimated spectrophotometrically. Briefly, 70 μl of double distilled water was added to 10 μl of lysate. Then, 50 μl of 50 mM phosphate buffer, 10 μl of 1 mM butylated hydroxy toluene (BHT), and 75 μl of 1.3% thiobarbituric acid (TBA) were added. The lipids were isolated by precipitating them with 50 μl of 50% trichloro acetic acid. The mixture was then incubated at 60 °C for 40 min and then kept on ice for 15 min. 10 μl of 20% sodium dodecyl sulphate was added to stop the reaction. The pink coloured MDA–TBA adduct formed was read at 530 nm with a reference wavelength of 630 nm serving as blank using a SpectramaxPLUS 384 (Molecular Devices, USA).

Superoxide dismutase (SOD) activity in the serum and liver homogenates was measured by the method described by Kakkar *et al.*[34] The SOD activity was measured spectrophotometrically by inhibition of a nitro blue tetrazolium dye-reduced NADH and phenazine methosulfate (PMS) system, leading to blue formazan formation. The reaction was started by adding NADH and stopped after 90 s by adding glacial acetic acid. Absorbance of the formazan product was monitored at 560 nm using a SpectramaxPLUS 384 microplate reader. Fifty percent inhibition of formazan formation in 1 min is considered as 1 unit SOD activity.

2.9 Western blotting

The hepatic tissues were homogenized in 10% wt/vol RIPA buffer with 0.1 mM protease (Cat no. P8340, Sigma) and phosphatase inhibitor cocktail (Cat no. P2850, Sigma). The homogenate was kept on ice for 20 min followed by centrifugation at 12 000*g* for 20 min at 4 °C. The supernatants were obtained, and the protein content was quantified by the BCA method.[35] Equal proteins (40–60 μg) were resolved by 10% SDS-PAGE and transferred onto PVDF membranes (Millipore). After 2 h of blocking by 1× blocking buffer (Sigma), the membranes were incubated with primary antibodies (1 : 1000) overnight at 4 °C. After washing three times with PBST (5 min each), the blotted membranes were incubated with appropriate HRP-conjugated secondary antibodies (1 : 2000) for 2 h at room temperature. The protein expression was detected with an Immobilon Western Chemiluminescent HRP substrate detection kit (Millipore, Cat. no. WBKLS0500) using an ImageQuant LAS 500 detection system (GE Healthcare, Upsala, Sweden). Data were presented as the ratios of the target protein to β-actin. The bands from western blotting were quantified using the ImageJ 1.47v software (National Institutes of Health, Bethesda, MD, USA). For each study, western blot analysis was performed three times and the representative blots are shown.

2.10 Immunohistochemistry

Briefly, the liver sections (5 μm) were cut from the paraffin blocks and sequentially deparaffinized with xylene. Antigen retrieval was performed by heating the slides in citrate buffer (10 mmol L^{-1}). The slides were incubated with the desired primary antibodies at 1 : 200 dilutions overnight at 4 °C. The slides were then rinsed gently three times with PBST followed by incubation for 4 h with fluorescently-labeled secondary antibodies. The nuclei were counterstained using Hoechst 33258 (1 mg ml^{-1}) for 5 min in the dark and were visualized using a fluorescence microscope (Nikon Eclipse 80i, Tokyo, Japan, and Life Technologies EVOS FL Auto).

2.11 Real-time polymerase chain reaction (RT-PCR)

Total hepatic RNA was extracted using RNA isoPLUS reagent following the manufacturer's protocol (Invitrogen, Carlsbad, CA, USA) wherein 1 ml of RNA isoPLUS was added to ~20 mg of hepatic tissue. First strand cDNA was prepared by using a Primescript™ 1st strand cDNA synthesis kit (TAKARA Bio Inc). RT-PCR was performed using TB Green™ Premix Ex Taq™ II (TliRNaseH Plus) in Quant studio 6 flex (Applied Biosystems, Thermo Fisher Scientific Inc.) and the expression fold changes were calculated using the comparative CT method. The primer sequences of specific genes are presented in Table 2. GAPDH was used as an endogenous reference gene to normalize the gene expression.

Table 2 Primer sequences used for real-time PCR

Gene	Forward	Reverse
ACC-1	5′-CTTGGGGTGATGCTCCCATT-3′	5′-GCTGGGCTTAAACCCCTCAT-3′
SREBP1-c	5′-GGAGCCATGGATTGCACATTTGA-3′	5′-CTGTGTCTCCTGTCTCACCCC-3′
LKB1	5′-CTTTGAGAACATCGGGAGAGG-3′	5′-CTGTGCTGTCTAATCTGTCGG-3′
FAS	5′AGGGGTCGACCTGGTCCTCA-3′	5′-GCCATGCCCAGAGGGTGGTT-3′
PPARα	5′-CCATCTGTCCTCTCTCCCCA-3′	5′-CCTCTCCGAGGGACTGAGAA-3′
SIRT1	5′-GACGACGAGGGCGAGGAG-3′	5′-ACAGGAGGTTGTCTCGGTAGC-3′
PPARγ	5′-GAACAGATCCAGTGGTTGCAG-3′	5′-GGCATTATGAGACATCCCCAC-3′
SCD1	5′-CCAACACAATGGCATTCCAG-3′	5′-GGTGGTCACGAGCCCATTC-3′
AMPK	5′-CAGGGACTGCTACTCCACAGAG-3′	5′-CCTTGAGCCTCAGCATCTGAA-3′
GAPDH	5′-GATTTGGCCGTATCGGAC-3′	5′-GAAGACGCCAGTAGACTC-3′

2.12 Transmission electron microscopy

The liver tissues were dissected into 1 mm^3 sections for morphological studies by transmission electron microscopy (TEM). The sections were washed twice with chilled 0.2 M sodium cacodylate buffer containing 0.1% calcium chloride, pH 7.4. The samples were then fixed in a mixture of 2% paraformaldehyde and 2.5% glutaraldehyde in 0.1 M sodium cacodylate buffer for 2 h at 4 °C. Thereafter, the fixed pellets were washed carefully with 0.1 M cacodylate buffer and post-fixed with 1% osmium tetraoxide for 2 h, followed by centrifugation. The samples were then dehydrated in acetone (15, 30, 60, 90, and 100%) and propylene oxide (twice for 10 min each), placed in Araldite and DDSA medium, and then heated at 65 °C for 48 h. The prepared sample blocks were cut using an ultramicrotome (Leica EM UC7, Vienna, Austria), mounted on the copper grids, and doubly stained with uranyl acetate and lead citrate. The stained samples were examined with a transmission electron microscope (TECNAI G2 SPIRIT, FEI, Netherlands) equipped with a Gatan Orius camera.

2.13 Immunoprecipitation

For each immunoprecipitation (IP) or co-immunoprecipitation (CO-IP), 500 μg of protein from hepatic tissue lysate prepared in NP-40 lysis buffer (20 mM HEPES, pH 7.4, 1% NP-40, 1 mM DTT and inhibitor cocktails) was utilized. Protein lysate was incubated with 20 μl of protein A–G (Santa Cruz Biotechnology) and 1–2 μg of primary antibodies: anti-rabbit SIRT1 and anti-rabbit LKB1 antibodies for 2 h at 4 °C using a tube rotator. The immunoprecipitates obtained were rinsed thrice with chilled PBS, and then heated with 2× SDS sample buffer. The immunoprecipitates were resolved by 10% SDS-PAGE, followed by immunoblotting against the respective antibody.

2.14 Pull down assay

Activation of sepharose 4B beads was performed according to the manufacturer's protocol. CNBr (300 mg) activated sepharose 4B beads were first suspended in 10 ml of 1 M HCl and then washed with 1 M HCl (10 times, 10 minutes per washing). Lastly, the swollen beads were rinsed with coupling buffer (0.1 M $NaHCO_3$, pH 8.3, 0.5 M NaCl). The medium was further divided into two: one was used as the blank and the other for berbamine coupling. 2 mg of berbamine was added and the final volume was made to 1.5 ml using coupling buffer. The suspension was rotated overnight at 4 °C followed by washing and blocking. Then, the beads were rinsed twice with reaction buffer (50 mM Tris, pH 7.5, 5 mM EDTA, 150 mM NaCl, 1 mM DTT, 0.01% NP-40, 2 mg ml^{-1} BSA, 0.02 mM PMSF and protease inhibitor cocktail). 100 μg of protein of hepatic lysate was incubated with 50 μl of BBM-conjugated and blank sepharose beads and rotated overnight at 4 °C. The pull-down protein was rinsed thrice with reaction buffer followed by boiling with the 2× SDS loading dye. The proteins were then resolved by 10% SDS-PAGE followed by their transfer onto PVDF membranes and probing with the desired proteins.

2.15 Quantitative monodansylcadaverine (MDC) staining

The autophagic flux in the control and treated rats were measured by using monodansylcadaverine (MDC).[36] In brief, 1- to 5 mm^3 tissue sample was minced in 1–2 mL of homogenization buffer and centrifuged at 1000*g* for 5 min at 4 °C to spin out the nuclei and heavy membrane. 25 μM MDC was added to the postnuclear supernatant fraction and incubated on ice for 10 min in the dark. The sample was centrifuged at 20 000*g* for 20 min at 4 °C and the pellet obtained was rinsed twice with 1 mL of cold resuspension buffer. The pellet was resuspended in 350 μL of resuspension buffer. 100 μL per well was used for measurement with a fluorescence plate reader (Varioskan Flash, Thermo Scientific) at an excitation/emission wavelength of 495/519 nm. The relative fluorescence units (RFUs) were calculated per mg of protein.

2.16 Oil Red O staining

The formalin-fixed liver tissue samples were embedded in paraffin and 5 μm sections were prepared using a rotary microtome (Leica RM 2155, Germany). The sections were mounted on glass slides, stained with Oil Red O (Sigma) and visualized using an inverted microscope (Nikon Eclipse Ti).

2.17 Statistical analysis

All experiments were repeatedly performed thrice and the data were expressed as mean value ± SD. Statistical comparisons between the mean values of different groups were performed by one-way analysis of variance (ANOVA). The H-BBM and HFD groups were compared with the control group, while the HFD-FF, HFD-LBBM and HFD-HBBM groups were compared with the HFD group. Differences were considered to be statistically significant when the P values were less than 0.05 ($P < 0.05$).

3. Results

3.1 Effects of BBM on the body weight and liver index

Rats fed with a high fat diet for 12 weeks had a marked increase in their body weights ($P < 0.001$) compared with the control group. BBM treatment at low (50 mg kg^{-1}) and high (150 mg kg^{-1}) concentrations for 28 days co-administered with HFD prevented gain in the body weight compared with the rats in the HFD group ($P = 0.11$ and $P = 0.11$ respectively) (Fig. 1A). Treatment with BBM (150 mg kg^{-1}) in control rats did not show much change in the body weight as compared with the control group. Therefore, the berbamine treatment to some extent prevented the weight gain caused by HFD in male Wistar rats.

Liver index (liver wet weight/body weight × 100%) is also an important attribute to be taken into consideration in NAFLD studies. At the end of the experimental period, it was observed that the HFD fed rats had a significant increase of 154% in the liver index as compared to the control group ($P < 0.001$). The BBM treated control group did not show any major change in the liver index, indicating that BBM had no adverse effect on the liver index. The BBM treated HFD group showed a dramatic

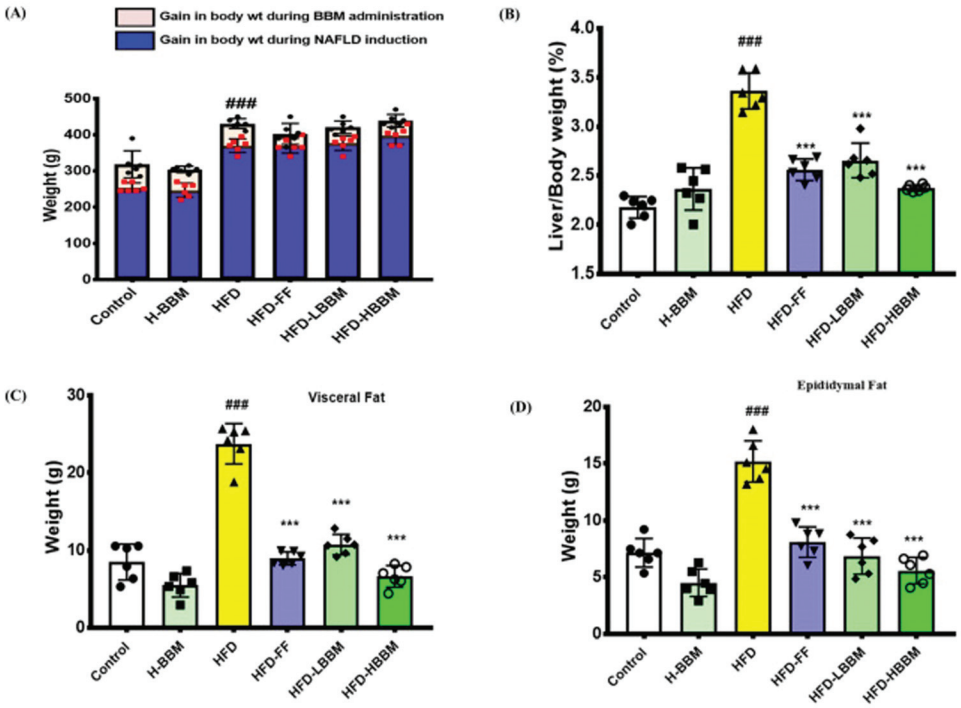

Fig. 1 Effects of berbamine on the body weight and liver index. Effects of BBM on body weight (A) and liver index (B). Reduction in the visceral (C) and epididymal fat (D) weight. Data are presented as mean ± S.D. (n = 6). #P < 0.05, ##P < 0.01 and ###P < 0.001 compared with the control group. *P < 0.05, **P < 0.01 and ***P < 0.001 compared with the HFD treated group.

decrease of 121.91% (P < 0.001) and 108.93% (P < 0.001) in the liver index at 50 and 150 mg kg^{-1} doses respectively (Fig. 1B).

It was observed that HFD fed rats showed a significant increase in their visceral (P < 0.001) and epididymal fat (P < 0.001) as compared to the control. On the other hand, BBM co-administered with HFD significantly ameliorated both the above-mentioned parameters to their normal levels (Fig. 1C & D). Fenofibrate, a drug of choice for the treatment of NAFLD, was also found to positively regulate the amelioration of visceral (P < 0.001) and epididymal fat (P < 0.001).

3.2 Berbamine mediated amelioration of liver function defects in HFD rats

In this experimental study, we observed that berbamine administration for 28 days had promising hepatoprotective effects. BBM treatment potentially modulates the inflammatory and oxidative stress biomarkers in liver tissues and serum lipids in HFD diet-induced NAFLD rats. AST, ALT and ALP are the liver specific enzymes which serve as the hallmarks of liver injury. Liver injury or dysfunction leads to alterations in the levels and/or activities of these enzymes which serve as the identification parameters (Table 3). In HFD-induced NAFLD rats, AST was released in excess in the serum of HFD rats as compared with the control group animals (P < 0.05). However, BBM supplementation reduced the AST activities when compared with HFD at both doses of 50 and 150 mg kg^{-1} (P < 0.05). This indicates the protective potential of BBM in improving the hepatic fibrosis conditions in chronic high fat diet fed rats. However, the levels of ALT and ALP were similar to a great extent across all treated groups.

Table 3 Assessment of serological parameters

Groups	Total protein (g dL^{-1})	Albumin (g dL^{-1})	Globulin (mg dL^{-1})	Albumin/ globulin ratio	Alkaline phosphatase (ALP) (U dL^{-1})	Aspartate transaminase (AST) (U dL^{-1})	Alanine transaminase (ALT) (U dL^{-1})
Control	5.09 ± 1.31	2.43 ± 0.65	2.30 ± 1.1	1058.364	58 ± 14.89	9.6 ± 2.65	35.5 ± 9.46
H-BBM	5.16 ± 0.79	2.13 ± 0.34	2.57 ± 0.38	832.0363	55 ± 13.41	10.85 ± 0.91	32.66 ± 10.96
HFD	3.72 ± 0.9	2.00 ± 0.41	2.73 ± 0.58	732.6431	58.3 ± 4.93	15.4 ± 1.27^{c}	34 ± 9.64
HFD-FF	5.82 ± 0.77*	2.99 ± 0.18	2.83 ± 0.64	1058.27	60.5 ± 5.06	10.6 ± 0.14*	36 ± 5.83
HFD-LBBM	5.68 ± 0.94 *	2.58 ± 1.58	3.37 ± 1.65	763.6902	54.4 ± 12.83	10.38 ± 1.79	32.6 ± 6.84
HFD-HBBM	5.95 ± 1.63*	3.54 ± 1.00	2.94 ± 0.99	1203.966	53 ± 16.46	8.8 ± 2.12*	38 ± 11.31

Data are presented as mean ± S.D. (n = 6). ^{a}P < 0.05, ^{b}P < 0.01 and ^{c}P < 0.001 compared with the control group. *P < 0.05, **P < 0.01 and ***P < 0.001 compared with the HFD treated group.

The liver dysfunction caused by HFD in the animals used in this study was again affirmed by assessing the alterations in the serum total protein content (Table 3) as it is established that NAFLD patients have altered amounts of serum proteins.[37] In this study, HFD fed NAFLD rats had lowered serum protein levels as compared with the control animals. The possible reason of impaired hepatic function may be lipid deposition. The most abundant circulatory serum protein is albumin. A healthy liver normally synthesizes albumin and any defect in the liver function leads to a defect in albumin synthesis. So, albumin level is also an important criterion to assess hepatic health.[38,39] Hypoalbuminemia, faulty albumin catabolism, was also observed in NAFLD animals. The NAFLD rats showed an increase in the globulin content, which seemed to be a compensatory mechanism. The albumin–globulin ratio was found to be lowered in the NAFLD rats, whereas it was found to be increased in the BBM administered NAFLD rats. Fenofibrate being the positive control drug against NAFLD showed improvement in the normal physiological aspects of liver function.

3.3 Effect of BBM on the serum and hepatic lipid profiles

The serum levels of total cholesterol (TC) and triglycerides (TG) in the HFD group were higher than those in the control group rats (all $P < 0.001$). However, the BBM treatment at both the doses reduced the serum TC and TG levels, when compared with the levels observed in the HFD group. The reduction in TG contents in the HFD-HBBM group was comparable to that in the positive control, HFD-FF group ($P < 0.001$).

Consistent with the changes in serum lipids, the hepatic lipid content was significantly upsurged in the HFD rats as compared with the control rats ($P < 0.001$), and these were decreased upon fenofibrate and BBM treatment. A downsurge of the hepatic glycogen content serves as a characteristic marker of hepatic insulin resistance (IR) which can lead to type-II diabetes.[40] The hepatic tissue of HFD rats had significantly depleted hepatic glycogen contents compared with the control rats ($P < 0.001$). After the BBM treatment, the rats showed a dramatic recovery of hepatic glycogen levels compared with the HFD rats ($P < 0.01$). Rats fed with a HFD had strikingly higher serum glucose levels than the normal control and BBM-control group animals. BBM treatment tends to lower the glucose levels (Table 4).

3.4 Effect of BBM on HFD-induced histological changes in NAFLD rats

The histological assessment of H&E staining showed that the livers of the HFD-fed rats showed increased lipid droplet deposition, acinar and portal inflammation, infiltration of macrophages and lymphocytes, clearly demonstrating the establishment of NAFLD (Fig. 2A). The other key histopathological features of NAFLD were also clearly visible in the sections demonstrating ballooning degeneration, altered architecture and vacuolated cytoplasm. The control animals administered only BBM also showed normal architectural features similar to those of the control animals, establishing the safety of berbamine at the highest level used in the present study. However, the NAFLD animals treated with BBM showed minimal steatosis and restoration of cellular architecture.

The assessment of the TEM micrographs of the liver sections to observe the ultrastructural changes in the liver architecture further validated the absence of necroinflammation or fibrosis. TEM analysis also showed significantly increased hepatic lipid content in HFD fed rats compared to the control rats. Interestingly, the BBM-treated rats exhibited little or no intrahepatic lipid droplet accumulation, even when fed with a HFD (Fig. 2B). The Oil Red O stained hepatic sections of different treatment groups also confirmed the above findings, showing the lipid accumulation inhibitory properties of BBM (Fig. 2C).

3.5 Effects of BBM on serum and hepatic oxidative stress

Oxidative stress plays a decisive role in the manner steatosis progresses to steatohepatitis.[41] Lipid peroxides are one of the reactive products generated as a result of uncontrolled ROS generation. These lipid peroxides damage the cellular machinery at the molecular level.[42] The lipid peroxidation (LPO) levels were found to be increased in the HFD fed NAFLD rats. However, the BBM administration at low and high concentrations in the NAFLD rats decreased the hepatic and serum LPO levels significantly (Fig. 3A and B). In the hepatic tissue, there was 0.62 ($P < 0.001$) and 0.52 ($P < 0.001$) fold decrease compared to HFD rats at 50 and 150 mg per kg body weight BBM doses, respectively, whereas in the serum there was 0.52 ($P < 0.001$) and 0.43 ($P < 0.001$) fold decrease compared to the control respectively.

SOD enzyme activity when assayed in the liver tissues and serum showed a downsurge in the HFD rats as compared with

Table 4 Effects of berbamine on the lipid profiles and glycogen contents

Groups	Serum cholesterol (mg dL^{-1})	Serum triglycerides (mg dL^{-1})	Hepatic triglycerides (mg g^{-1})	Hepatic glycogen (mg g^{-1})	Serum glucose (mg dL^{-1})
Control	26.67 ± 3.51	23.77 ± 11.92	55.52 ± 7.21	2.44 ± 0.2	46.25 ± 6.5
H-BBM	28.6 ± 3.64	35.77 ± 6.43	49.38 ± 5.94	1.97 ± 0.1	50.25 ± 3.5
HFD	44 ± 4.83^{c}	80.63 ± 12.88^{c}	92.74 ± 3.75^{c}	1.21 ± 0.03^{c}	87.33 ± 6.02^{b}
HFD-FF	37.67 ± 1.15	42.73 ± 13.58***	58.88 ± 3.10***	1.78 ± 0.19	65.6 ± 8.56
HFD-LBBM	40.33 ± 4.04	75.05 ± 6.41	77.17 ± 4.61***	1.76 ± 0.4	81.5 ± 17.46
HFD-HBBM	34.67 ± 4.93	59.13 ± 4.76	68.43 ± 5.15	1.98 ± 0.12**	90 ± 25.71

Data are presented as mean ± S.D. ($n = 6$). $^{a}P < 0.05$, $^{b}P < 0.01$ and $^{c}P < 0.001$ compared with the control group. $*P < 0.05$, $**P < 0.01$ and $***P < 0.001$ compared with the HFD treated group.

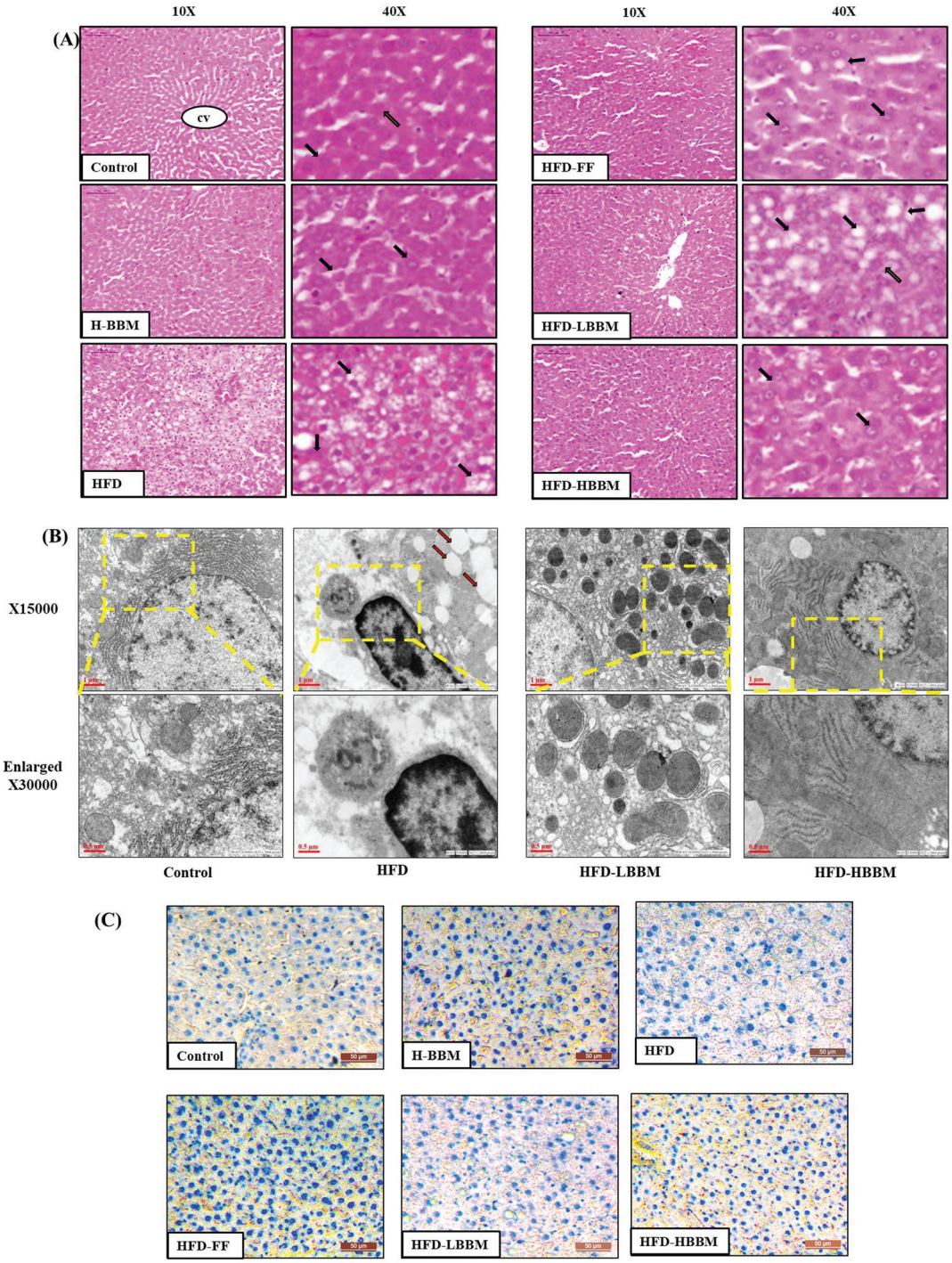

Fig. 2 Effects of berbamine on aggravation of structural liver damage. (A) Representative microscopic photographs of the liver sections stained with hematoxylin–eosin (magnification: 10× and 40×). (B) Transmission electron microscopy (TEM) ultrastructural analysis of liver samples from control, HFD and berbamine administered HFD rats. Two magnifications are shown for each sample (×15 000 and ×30 000). The data demonstrate the absence of necroinflammation or fibrosis and uncover the morphological differences between different treatment groups. (C) Representative microscopic photographs of the liver sections stained with Oil Red O (magnification: 20×) (n = 3).

the control rats ($P < 0.001$ and $P < 0.001$ respectively). However, the SOD activity was found to be increased in the BBM administered NAFLD rats (Fig. 3C & D). Fenofibrate also decreased lipid peroxidation and increased the SOD activity in the hepatic tissue and serum. The progression of hepatic steatotis also causes damage to cellular biomolecules which also affect antioxidant enzyme functions such as HO-1 and SOD-2. The immunoblots of HO-1 showed decreased levels in the HFD rats whereas the BBM administered HFD rats showed increased HO-1 levels in the hepatic tissue (Fig. 3E and F). BBM adminis-

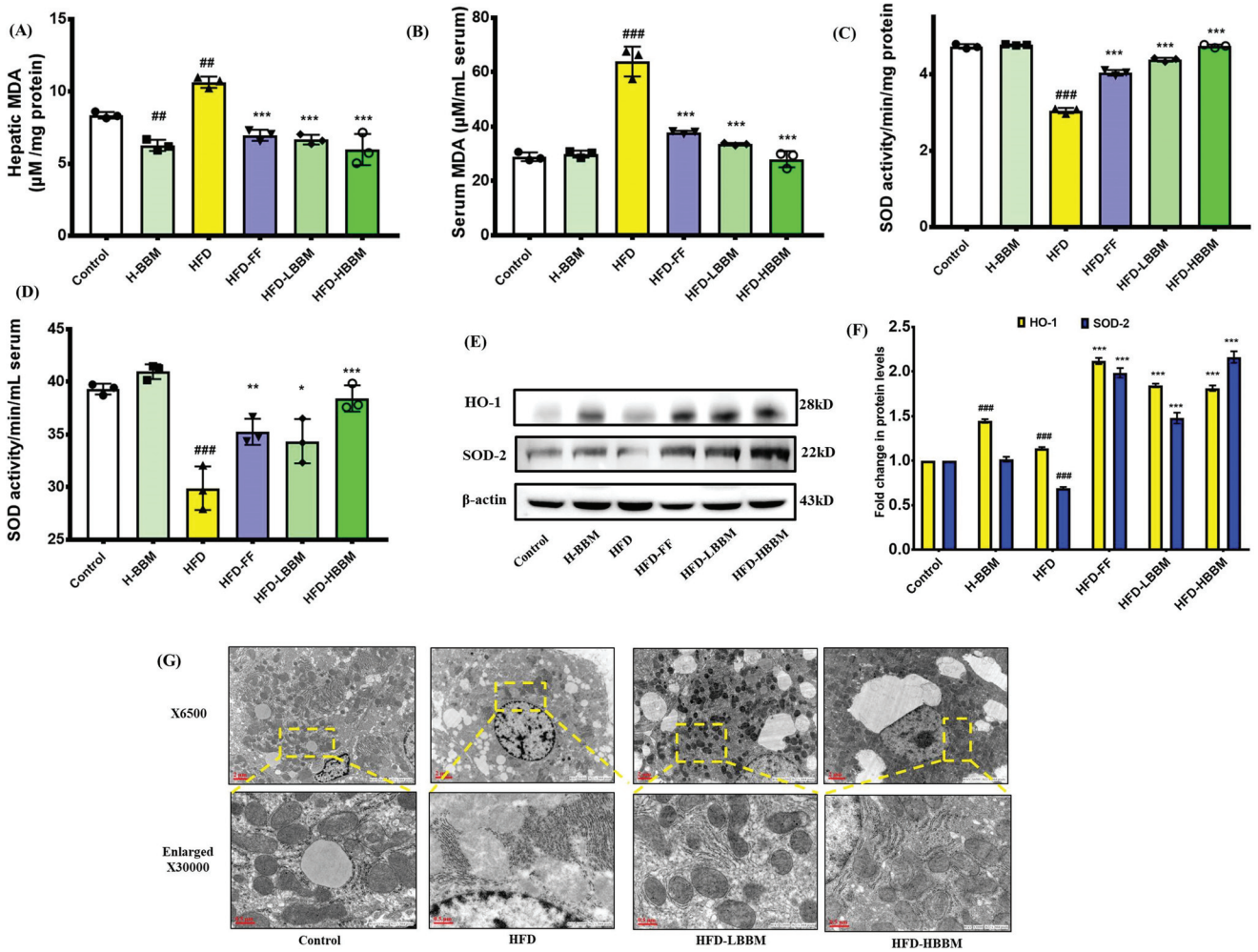

Fig. 3 Effects of berbamine on oxidative stress. Bar graphs represent the amount of MDA generated in (A) the hepatic tissue and (B) serum. SOD activity is expressed in (C) the hepatic tissue and (D) serum. (E) Immunoblots of SOD-2 and HO-1 proteins. β-Actin served as the loading control. (F) The bar graph shows the densitometric analysis of SOD-2 and HO-1. (G) TEM micrographs showing the ultrastructural changes in mitochondria of the hepatic tissue of control, HFD and berbamine administered HFD rats (magnification: ×6500, ×30 000, ×52 000 and ×67 000). Data are presented as mean ± S.D. (n = 3). #P < 0.05, ##P < 0.01 and ###P < 0.001 compared with the control group. *P < 0.05, **P < 0.01 and ***P < 0.001 compared with the HFD treated group.

tered HFD rats showed a marginal increase in the SOD levels as compared to HFD rats. The HO-1 levels in the H-BBM group were similar to those in the control whereas the SOD-2 levels were found to be elevated (P < 0.001) owing to the antioxidant properties of berbamine. Mitochondria plays an integral role in HFD-induced oxidative stress which is a physiological attribute of NAFLD pathogenesis. The TEM images of the hepatic tissue of NAFLD rats showed disrupted integrity of mitochondria with dissolved cristae (Fig. 3G). However, the treatment with BBM improved the normal physiological architecture of mitochondria indistinct from the control.

3.6 BBM regulates hepatic lipid metabolism *via* the SIRT1/LKB1/AMPK signaling pathway

SIRT1 is a TYPE III NAD-dependent deacetylase that acts as a metabolic sensor of NAD^+ which regulates cellular metabolism.[43] SIRT1 also regulates hepatocellular lipid metabolism.[44] To further delineate the potential role of SIRT1 in modulating BBM mediated lipid metabolism the expression profiling of SIRT1was studied at the protein and mRNA levels. The protein levels of SIRT1 were increased in the H-BBM group (P < 0.001) when compared to the control, showing the SIRT1 upregulating potential of BBM, whereas in the HFD-fed rats the protein levels were decreased (Fig. 4A & B). Concurrent administration of BBM increased the SIRT1 protein levels in HFD rats. The mRNA expression levels of SIRT1 were also assessed in the hepatic lysate of all treatment groups. In accordance with the western blot data, the mRNA levels of SIRT1 were also increased in the H-BBM group. By comparing the mRNA levels of SIRT1 in the hepatic tissue of HFD rats, it was observed that BBM administration increased the SIRT1 mRNA levels at both the doses of 50 mg kg^{-1} (P < 0.05) and 150 mg kg^{-1} (P < 0.01) (Fig. 4C). The pull-down assay further confirmed the direct interaction of BBM with SIRT1 in

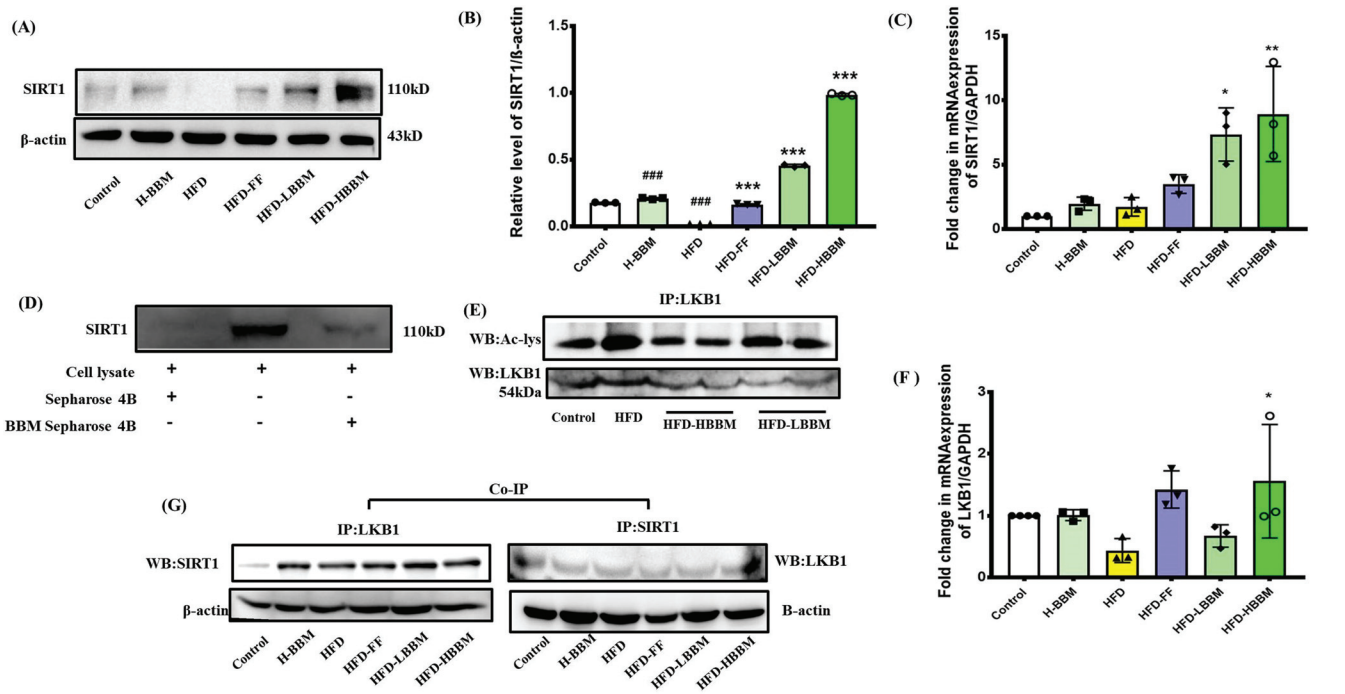

Fig. 4 Berbamine activates the SIRT1/LKB1 pathway in NAFLD rats. (A) The dose–response effect of BBM on SIRT1 protein levels in the hepatic tissue of control, HFD and BBM/fenofibrate treated HFD rats. β-Actin served as the loading control for western blot. (B) Bar graph represents the densitometric analysis of SIRT1/β-actin. (C) The mRNA expression levels of SIRT1 in control, HFD and BBM/fenofibrate treated HFD rats. GAPDH served as an endogenous control in mRNA analysis. (D) Western blot of SIRT1 demonstrating its interaction with berbamine as observed through the pull-down assay. Proteins coupled with BBM were precipitated using activated CNBr-sepharose beads followed by immunoblotting. (E) IP of acetylated liver kinase B1 (LKB1). (F) The bar graph represents the mRNA expression levels of LKB1 using GAPDH as an internal control in the control and treated groups. (G) Co-immunoprecipitation study showing the interaction between SIRT1 and LKB1. Data are presented as mean ± S.D. (n = 3). #P < 0.05, ##P < 0.01 and ###P < 0.001 compared with the control group. *P < 0.05, **P < 0.01 and ***P < 0.001 compared with the HFD treated group.

NAFLD induced rats (Fig. 4D). The acetylation levels of LKB1 was measured by IP to establish the BBM-mediated SIRT1 deacetylase activity. As presented in Fig. 4E, BBM significantly decreased LKB1 acetylation upon normalization with protein input. The mRNA levels of LKB1 were found to be decreased in the HFD rats and were subsequently increased in the BBM administered HFD rats (Fig. 4F). To assess the interaction between SIRT1 and LKB1, co-immunoprecipitation of total tissue lysate was performed. It was observed that SIRT1-LKB1 was co-immunoprecipitated from total tissue lysate which affirms that berbamine induced activation of SIRT1 which directly interacts with LKB1 in HFD rats (Fig. 4G). These findings confirmed the interaction between SIRT1 and LKB1in BBM administered HFD rats.

To investigate the BBM mediated effects on the AMPK signaling pathway, we assessed the effects of BBM on phosphorylation of AMPK. The HFD rats showed a 0.83 fold decrease in the mRNA levels of AMPK compared to the control rats (Fig. 5A). The HBBM-HFD group showed a 7.36 fold increase in the mRNA levels of AMPK compared to the control (P < 0.001). The immunoblotting data show that HFD-fed rats had significantly subsided levels of the phosphorylated form of AMPK (Thr 172) (P < 0.001). However, the BBM administered rats showed notably increased phosphorylation levels of AMPK (P < 0.001) as assessed by immunoblotting (Fig. 5B & C). The immunohistochemistry images also showed decreased P-AMPK levels in HFD rats and these levels tend to increase upon BBM administration (Fig. 5D and E). Several studies have reported that polyphenols trigger AMPK activation indirectly,[45] suggesting the involvement of upstream kinase LKB1 in mediating the effect of SIRT1 on AMPK. mTORC1, being an immediate downstream effector molecule of AMPK, plays an important role in the regulation of lipid metabolism during the pathogenesis of NAFLD. The phosphorylated form of mTOR (Ser2448) was lowered at the protein levels as evident from the immunoblots (Fig. 5F and G), which established the possible involvement of mTOR in berbamine-administered HFD rats. These findings revealed that BBM mediated SIRT1 activation up-regulated the AMPK signaling cascade through LKB1 deacetylation in the liver. BBM mediated activation of the SIRT1/LKB1/AMPK signaling pathway plays a regulatory role in hepatic lipid metabolism.

3.7 BBM regulates the distribution of SREBP-1c and expression of lipid metabolic regulators in the liver

SREBP-1c is a membrane-binding protein located on the surface of the endoplasmic reticulum membrane that controls lipid metabolism-related enzymes.[46] The protein expression of SREBP-1c in HFD rats was higher than that in control rats (Fig. 6A & B). The immunohistochemistry images show the

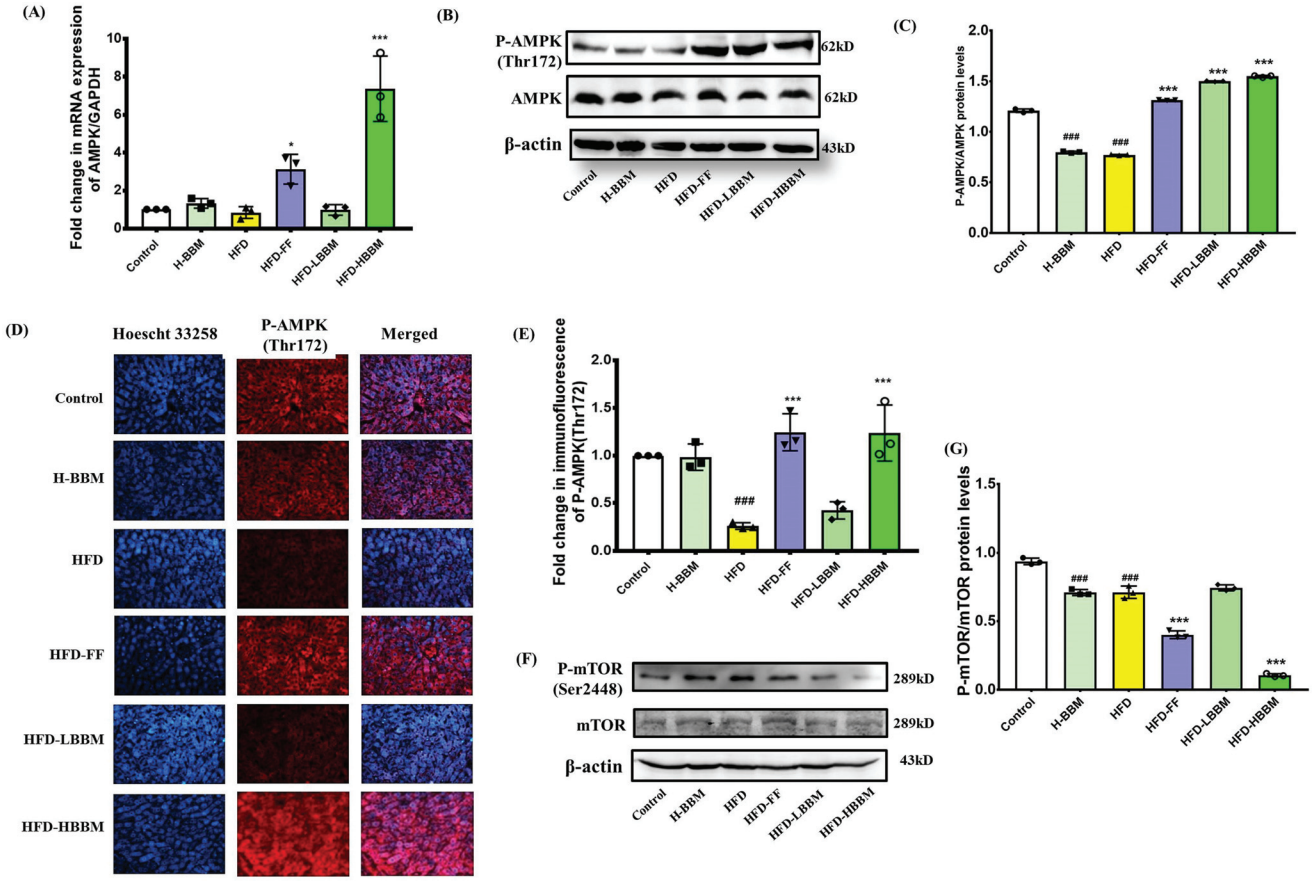

Fig. 5 Pharmacological activation of AMPK *via* the SIRT1/LKB1 axis. (A) Bar graph represents the fold change in the mRNA levels of AMPK of control and treated animals. (B) Representative immunoblotting analysis with antibodies against AMPK phosphorylated at Thr172 (P-AMPK) and total AMPK respectively, is shown. β-Actin served as the loading control. (C) The bar graph represents the densitometric ratio of P-AMPK/AMPK. (D) Immunohistostaining of the P-AMPK protein in the liver tissue section (magnification: 40× and scale bar: 100 μm). (E) The bar graphs show the mean fluorescence intensity of P-AMPK. (F) Representative immunoblots with antibodies against mTOR and P-mTOR (Ser2448). (G) The bar graph represents the densitometric ratio of P-mTOR/mTOR. Data are presented as mean ± S.D. (n = 3). #P < 0.05, ##P < 0.01 and ###P < 0.001 compared with the control group. *P < 0.05, **P < 0.01 and ***P < 0.001 compared with the HFD treated group.

increased expression of SREBP-1c in the HFD rats which was ameliorated by BBM (Fig. 6C and D). Fenofibrate treatment also decreased the SREBP-1c expression in HFD rats. The mRNA expression of SREBP-1c was also increased in HFD rats (P < 0.001) (Fig. 6E). BBM administration was found to reverse these changes significantly. These findings suggest that BBM might repress the transcription of genes involved in lipid synthesis by downregulating the expression of SREBP-1c through SIRT1/LKB1/AMPK signaling.

To delineate the mechanism of action of BBM in inhibiting lipid deposition in the liver, we assessed lipid metabolism regulatory enzymes. As shown in Fig. 7, the expression of several lipid synthesis-associated enzymes changed across the treated groups. In the way of *de novo* synthesis, the levels of fatty acid synthase (FAS; P < 0.001) and steroylCoA desaturase (SCD1; P < 0.001) were significantly increased in the HFD rats (Fig. 7A). The mRNA expressions of FAS and SCD1 in conjunction with the immunoblotting data *i.e.* the corresponding protein levels were alleviated in the BBM administered HFD rats (Fig. 7B). PPAR-α is an imperative transcription factor that regulates several aspects of hepatic lipid metabolism to maintain fatty acid homeostasis.[47] PPAR-α was found to be decreased in the HFD rats as assessed at the protein (Fig. 7C) and mRNA levels (Fig. 7D). However, BBM administration tends to increase PPAR-α expression at both the doses. In hepatocytes, PPAR-γ is a transcriptional regulator of lipid metabolism that targets genes involved in FFA import and *de novo* lipogenesis (DNL).[48] The expression of PPAR-γ was increased in HFD fed rats at the protein and mRNA levels but it tended to decrease upon BBM administration in the HFD rats. Acetyl CoA carboxylase is a key modulator of hepatic lipogenesis that catalyzes the carboxylation of acetyl-CoA to produce malonyl-CoA. The phospho-ACC (Ser79) levels were also increased by BBM as compared with the ACC levels (Fig. 7E & F). The mRNA level of ACC1 was also decreased in HFD rats (P < 0.001) which improved upon BBM treatment (P < 0.001) (Fig. 7G). The expression of the scavenger receptor CD36 that mediates the recognition and internalization of lipids was decreased in HFD

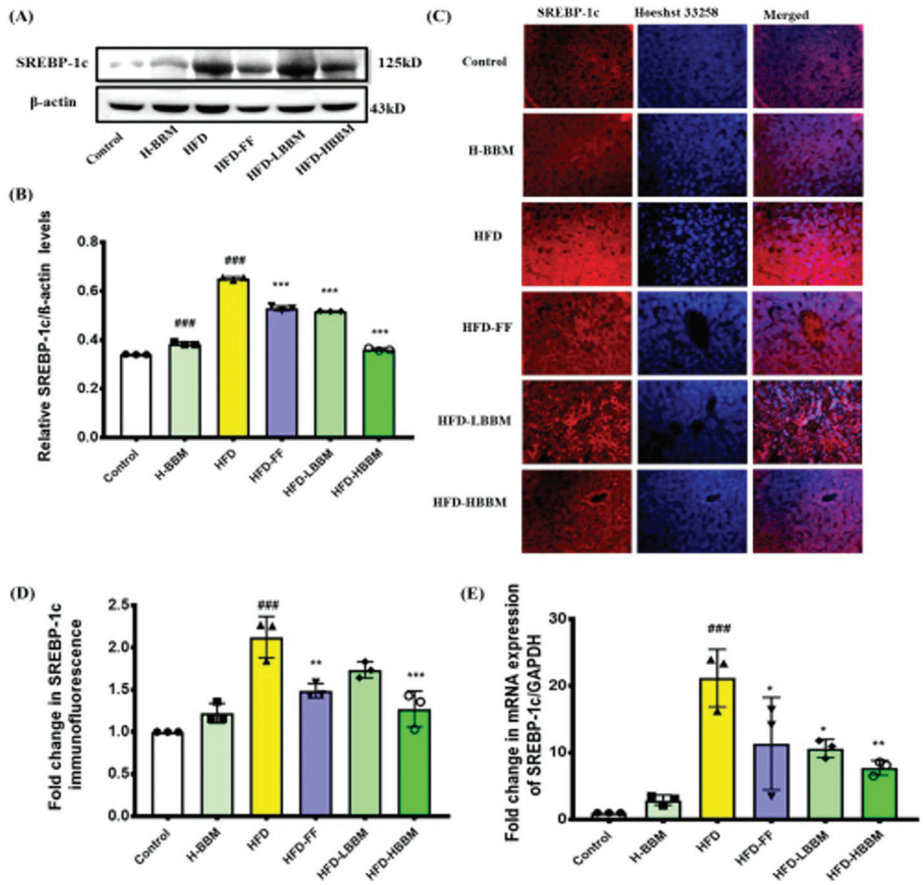

Fig. 6 Berbamine causes diminution of transcription factor SREBP-1c *via* the SIRT1/LKB1/AMPK signaling pathway. (A) Representative immunoblotting analysis with antibodies against SREBP-1c is shown. β-Actin served as the loading control. (B) The bar graph represents densitometric analysis of SREBP-1c/β-actin. (C) Immunohistostaining of the SREBP-1c protein in the liver tissue section (magnification: 40× and scale bar: 100 μm). (D) The bar graphs show the mean fluorescence intensity of SREBP-1c. (E) Bar graph represents the fold change in the mRNA levels of SREBP-1c/GAPDH of control and treated animals. Data are presented as mean ± S.D. (n = 3). #P < 0.05, ##P < 0.01 and ###P < 0.001 compared with the control group. *P < 0.05, **P < 0.01 and ***P < 0.001 compared with the HFD treated group.

rats but was upsurged by BBM. Berbamine also decreased ChREBP-α expression which was found to be increased in HFD rats (Fig. 7H). These results suggest that berbamine could promote free fatty acid uptake and oxidation and inhibit the synthesis of FFA and TG by regulating the expression of key enzymes in NAFLD rats.

3.8 BBM restored the impaired hepatic autophagy in NAFLD rats

Autophagy which plays an imperative role in regulating lipid metabolism is dysregulated in various liver diseases. The clearance of excessive lipid droplets (LDs) is prevented due to impaired autophagy, which also leads to the development and progression of non-alcoholic fatty liver disease. Chronic lipid insult suppresses the SIRT1-mediated autophagic pathways in hepatocytes, decreasing the autophagic activity and resulting in the accumulation of intracellular lipids.[49] In this study, an autophagy marker protein, LC3A/B, was monitored to indicate the procession of autophagy. The immunoblotting data showed a decrease in the LC3A/B levels in the HFD rats when compared with the vehicle control. Our results showed that berbamine administration upregulated the LC3A/B protein level, which suggests the involvement of autophagy in the TG breakdown process (Fig. 8A & B). The effects of BBM administration on the expression of various autophagy-related proteins, including Beclin 1 and p62 were also assessed. The expression level of Beclin 1 was also found to be decreased in the HFD rats (P < 0.05). However, in the BBM administered HFD rats the protein levels were found to be increased as compared to the HFD rats (P < 0.001). The levels of p62 (the selective substrate for autophagy) were found to be increased in the HFD rats but were downsurged in the BBM administered HFD rats (Fig. 8A & B). Furthermore, immunohistochemistry analysis also confirmed the increase in the protein levels of LC3B upon BBM administration in HFD rats. These findings indicate that the mechanism of BBM induced restoration of autophagic flux is *via* the SIRT1/AMPK signaling axis in HFD rats (Fig. 8C). To selectively assess the increase in the number of autophagosomes, the fluorimetric analysis of monodansylcadaverine-stained hepatic tissue was performed. The monodansylcadaverine liver represents an accurate indicator of autophagic flux, as it only labels autophagosomes that have fused with lyso-

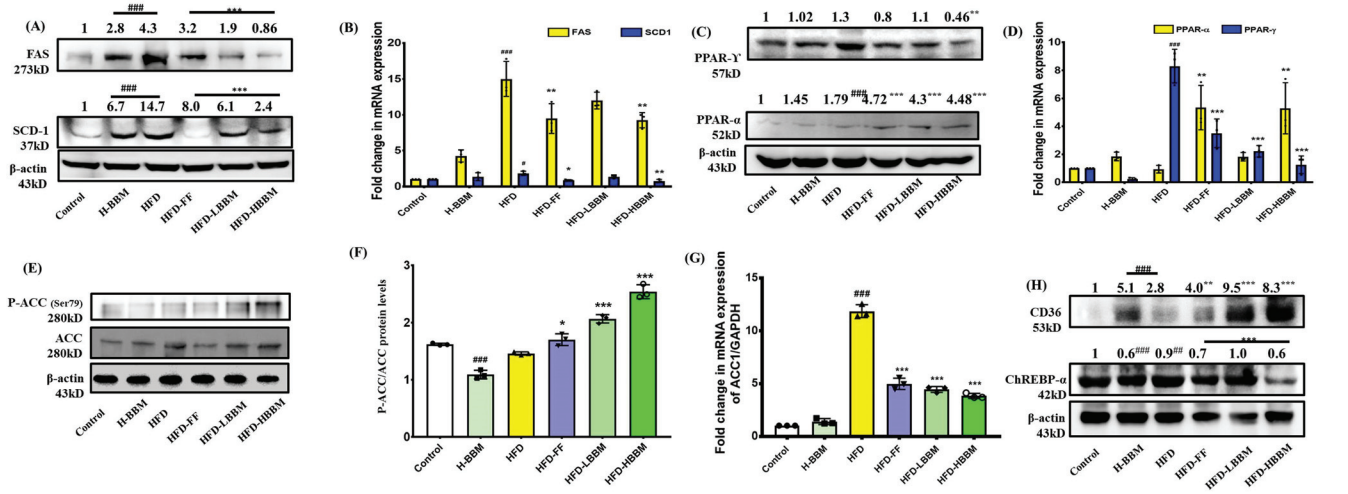

Fig. 7 Effect of berbamine on the expression of lipid metabolic regulators in the liver. The protein levels (A) and mRNA expression (B) of fatty acid synthase (FAS) and steroylCoA desaturase 1 (SCD1) in the hepatic tissue of different treated groups. Alterations in the PPAR-α and PPAR-γ expression levels were assessed at the protein levels by immunoblotting (C) and at the mRNA levels (D). GAPDH served as an endogenous control in mRNA analysis and β-actin served as the loading control for western blot. (E) Representative immunoblotting analysis with antibodies against P-ACC (Ser 79) and ACC respectively are shown. β-Actin served as the loading control. (F) The bar graph represents the densitometric ratio of P-ACC/ACC. (G) The bar graph represents the fold change in the mRNA levels of ACC1. (H) Immunoblots depicting the expression of ChREBP-α and CD36. Data are presented as mean ± S.D. (n = 3). #P < 0.05, ##P < 0.01 and ###P < 0.001 compared with the control group. *P < 0.05, **P < 0.01 and ***P < 0.001 compared with the HFD treated group.

somes. MDC fluorescence was quenched in the NAFLD rats as compared with the control rats, whereas it was replenished after BBM administration in HFD rats (Fig. 8D). The histological results showed that BBM ameliorated fat infiltration in the liver, proposing that autophagy induced by BBM potentially facilitated the disruption of lipid droplets and also probably mitigated lipid droplet formation. As shown in Fig. 8E, TEM assays divulged the ultra-structural changes in the hepatic tissues of control and treated rats. Regarding the HFD group, the number of lipid droplets were found to be decreased in the hepatic tissue of BBM administered HFD rats. The macroautophagy induction is prominently shown by the red arrows. Taken together, these results suggested that BBM administration reinstated autophagy *via* the induction of SIRT1 and activation of AMPK in NAFLD rats.

4. Discussion

Obesity, a multifarious state caused due to prolonged intake of excess energy consumption, is an important aspect of the onset of various metabolic disorders such as NAFLD. Therefore, the development of new drugs for the management of obesity and NAFLD is the need of the hour. An animal model for the study of NAFLD can be developed either by genetic mutations[50] or by dietary[51] or pharmacological modifications.[52] Several recent studies have shown that long term feeding of rats with a high fat diet (standard rat chow added with 2% cholesterol and 15% lard) provides the experimental model of NAFLD as caloric overconsumption plays a major role in the development of the disease.[53] Previous reports state that in three days the rats fed with a high-fat diet develop hepatic insulin resistance preceding peripheral insulin resistance.[54] Different strategies are adopted for the management of this condition. The chemically synthesized drugs are often associated with some underlying toxic manifestations and harmful side-effects. Thus, herbal constituents are being explored by many researchers using NAFLD models to study their beneficial effects especially antioxidant capacity.[55] In-depth studies are necessitated to reconnoitre whether therapeutic agents of natural herbal origin with potential antioxidant and anti-inflammatory properties are efficient to cause recuperation of NAFLD.

In previous studies, it was observed that rats fed with a HFD for a long-term had liver injury which was accompanied by increased levels of serum TC, TG, FFA, ALT and AST compared with the rats fed a standard chow diet.[56] In our study, the HFD rats showed typical hepatic lesions which include hepatocyte ballooning, steatosis and hepatomegaly. The HFD fed rats also showed increased levels of TC, TG, ALT and AST as compared with the normal chow-fed control rats which are also the hallmarks of hepatic injury. These results indicated that HFD caused the development of dyslipidemia, steatosis and altered liver functions, suggesting the successful establishment of NAFLD animal model. However, BBM treatment significantly reduced the elevation of serum TG, TC, ALT, and AST and also hepatic lipids. In addition, the NAFLD induced histopathological alterations were also ameliorated by berbamine. The visceral and epididymal adipose tissue weight was also decreased upon BBM treatment.

The onset of NAFLD pathogenesis is also associated with the compromised antioxidant defense system of the body. The increased levels of free fatty acids and triglycerides induce lipo-

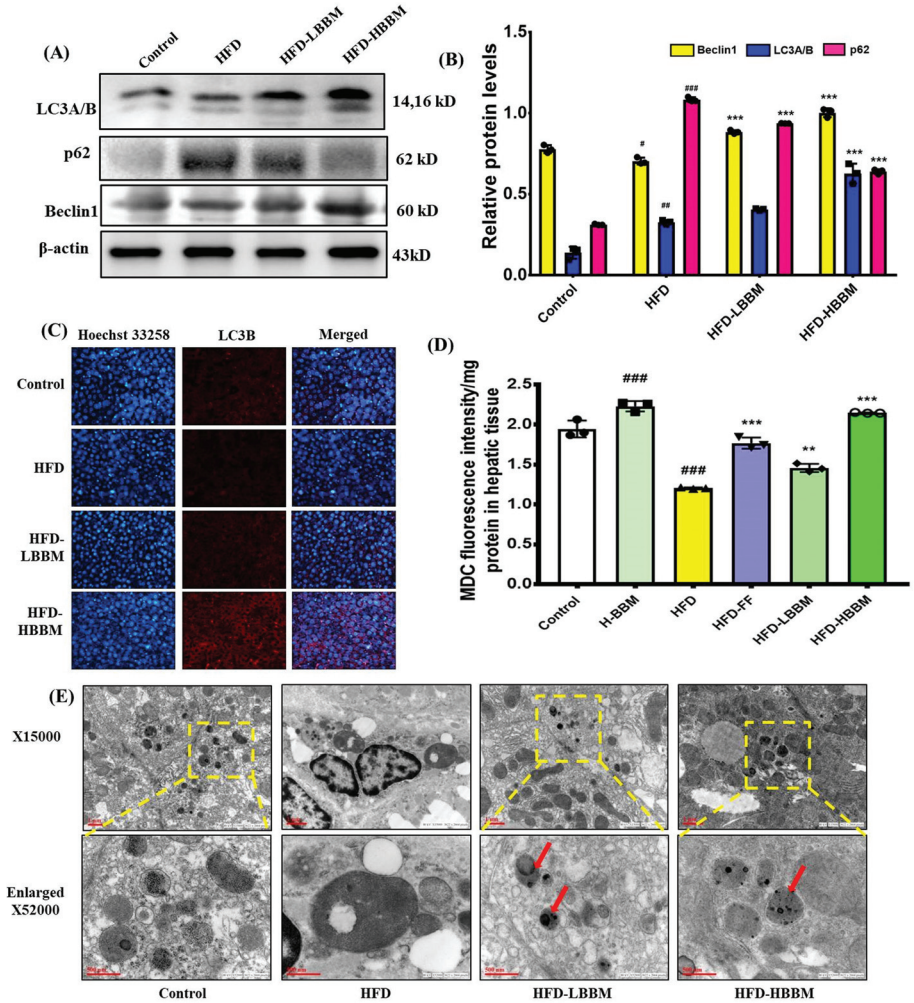

Fig. 8 Effects of berbamine on autophagy in NAFLD rats. (A) Effects of berbamine on the protein levels of the autophagic markers (LC3A/B, Beclin 1, and p62) in the hepatic tissue of control, HFD and berbamine administered HFD rats were assessed by immunoblotting. β-Actin served as the loading control for western blot. (B) The bar graph represents densitometric analysis of autophagic marker proteins. (C) Representative immunofluorescence micrographs of LC3B immunostained hepatic tissue are shown. (D) Bar graph represents the monodansylcadaverine fluorescence per mg protein in the hepatic tissue. (E) Effects of BBM on autophagy induction in the NAFLD liver was assessed by the TEM assay (magnification: ×15 000 and ×52 000). Data are presented as mean ± S.D. (n = 3). #P < 0.05, ##P < 0.01 and ###P < 0.001 compared with the control group. *P < 0.05, **P < 0.01 and ***P < 0.001 compared with the HFD treated group.

toxicity and oxidative stress which lead to hepatic inflammation, mitochondrial dysfunction, apoptosis, and fibrosis.[57] The present study also showed that the HFD group animals had an increased TBARS level in both serum and hepatic tissues, which is a characteristic marker of oxidative damage. BBM exhibited its antioxidant capacity by increasing the SOD activity, one of the principal scavenger of ROS and lowering the TBARS levels in serum and hepatic tissues. Heamoxygenase-1 (HO-1) which is another key antioxidant was decreased in the HFD rats. However, BBM administration upregulated the levels of HO-1, also establishing the positive influence of BBM treatment in maintaining the antioxidant status against NAFLD induced stress.

In recent years, various reports have shown that SIRT1 and AMPK are the two critical signaling targets controlling hepatic lipid metabolism. AMPK is a trimeric protein that serves as a cellular metabolic sensor and regulator under various stress conditions and functions to maintain the whole body energy balance.[58] SIRT1, an NAD-dependent deacetylase, is the most extensively studied sirtuin that has a prominent role in metabolic tissues, such as liver, skeletal muscle, and adipose tissues.[59] LKB1 is the principal AMPK kinase that catalyzes the phosphorylation of its catalytic α-subunit.[60] The present study aimed to study the activating potential of BBM by increasing the SIRT1 deacetylase activity, LKB1 deacetylation and phosphorylation mediated AMPK activation in NAFLD rats. HFD fed rats treated with berbamine expressed upsurged levels of SIRT1 and P-AMPK (Thr 172) in the hepatic tissue, whereas their levels were lowered in the NAFLD rats. SIRT1 activation was found to lower the lysine acetylation of LKB1, which causes its own activation and ultimately that of AMPK.[61] This study also showed that BBM stimulated AMPK phosphoryl-

ation and upsurged the expression of LKB1 in the hepatic tissue of HFD fed rats. The activation of SIRT1 has also been shown to upregulate SOD which ameliorates oxidative stress.[62] This could also be a possible mechanism by which BBM mediates its anti-oxidant properties by increasing the SOD activity.

Previous studies reported that AMPK phosphorylation can suppress the expression of various lipogenesis-related transcription factors which primarily include SREBP-1c.[63] SREBP-1c is the master regulator of the pathogenesis of metabolic disorders, including fatty liver, and serves as the most worked upon therapeutic target. According to various reports, it is well evident that AMPK activation inhibits SREBP-1c.[28,64] Regulation of hepatic SREBPs *in vivo* is dynamically regulated in response to nutritional and hormonal cues. Under fasting conditions, AMPK activation reduces lipogenesis in the liver by suppressing the SREBP-1c activity whereas inhibition of AMPK leads to the activation of SREBP-1c-mediated lipogenesis.[63] In this study, the HFD rats had significantly increased SREBP-1c which was ameliorated after BBM administration. AMPK activation also recruits mTOR which primarily regulates lipid metabolism by directly affecting SREBP-1c.[69] In the present study, mTOR was also found to be negatively regulated by AMPK activation in BBM administered NAFLD rats.

Our study also demonstrated that BBM treatment significantly reduced lipid accumulation in hepatic tissues in HFD animals. Therefore, to divulge the mechanism involved in its action, we assessed the regulation of several enzymes and genes involved in lipid metabolism. SREBP-1c is an imperative transcription factor which regulates several genes involved in the lipogenesis pathway, such as fatty acid synthase (FAS) and steroyl coA desaturase 1 (SCD1). BBM administration significantly lowered the hepatic expression of FAS and SCD1. These findings indicated that BBM exhibited its protective effect against NAFLD by suppressing lipid synthesis. PPARα and PPARγ are the two isotypes of PPAR which are expressed in a tissue specific pattern. They control many biological functions most importantly the lipid homeostasis in different tissues, including the liver.[65] Furthermore, PPAR-α, a nuclear hormone receptor, is a key component in the development of lipid disorders because of its central regulatory role in hepatic glucose and lipid metabolism. It plays an essential role in lipid transport and lipoprotein metabolism by promoting mitochondrial and peroxisomal fatty acid uptake and oxidation. In this study, we found that the PPAR-α protein and mRNA expression were lower in the livers of HFD rats. High fat-induced NASH susceptibility is eventually increased upon PPAR-α inhibition. Increase in PPAR-α expression could be the downstream effector of BBM action in improving fatty acid β-oxidation. PPAR-γ and ChREBP, the two key transcription factors which regulate lipogenesis and carbohydrate metabolism respectively, were also found to be upsurged in HFD rats. ACC1 is a principal lipid metabolizing enzyme that catalyzes acetyl CoA to produce malonyl-CoA for elongated fatty acid chains. Interestingly, ACC1 is activated by dephosphorylation, whereas phosphorylation switches it off.[66] ACC is the principal downstream target of activated AMPK which in turn causes its phosphorylation making it inactive. Our results also demonstrate that BBM administration reduces total cholesterol and triacylglycerol in serum and also lowers the hepatic adipogenesis through increased phosphorylation of ACC to regulate fatty acid synthesis. CD36 is the rate-limiting enzyme that facilitates the transport of plasma FFA into the liver at rest.[67] We found that CD36 is involved in the increased uptake of FFA in the hepatic tissue of HFD rats supplemented with BBM, a conclusion that is supported by the increase of CD36 protein expression. Thus, we propose that the protective effects of berbamine against hepatic steatosis in high fat-fed rats are mediated by the regulation of lipid homeostasis. Berbamine induced the activation of AMPK *via* the SIRT1/LKB1 axis which regulated several lipid related genes/proteins.

Autophagy, an intracellular degradation pathway, is indispensable for the maintenance of energy and cellular homeostasis.[68] Primarily it is recognized for the degradation of dysfunctional proteins and unwanted organelles; however, in recent years, several studies have also regarded lipid as one of the autophagy substrates.[70] Perturbations of autophagic flux have been suggested to contribute to various disease aetiologies, one among which is NAFLD. Our present study provided evidence for autophagosome formation induced by BBM as assessed by transmission electron microscopy. LC3A/B and Beclin 1 are the established markers for autophagy and p62/SQSTM1 is the selective substrate for autophagy and a marker for autophagic flux. Beclin 1 and LC3A/B expressions were upregulated by the phytochemical, whereas p62 being a negative regulator was downsurged upon BBM administration. These outcomes indicate that BBM mediated induction of autophagy should be considered as a novel approach for alleviating NAFLD mediated complications.

5. Conclusions

In succinct, we showed that the oral administration of BBM effectively reduced the body weight, together with resisting oxidative stress and lowering serum lipids and the biomarkers of hepatic injury. BBM also alleviated hepatic fat accumulation and decreased the hepatic triglyceride contents through modulation of the lipid metabolism machinery by regulating SREBP-1c and their downstream lipogenic targets *via* the activation of the SIRT1/LKB1/AMPK pathway. The beneficial metabolic effects of berbamine supplementation also include the regulation of SIRT1 mediated autophagy induction and its downstream processes. Consequently, we suggest that BBM can induce alterations in these liver metabolic pathways, which can be considered as an efficient strategy for the management of NAFLD.

Funding

This work was supported by grants from the Council of Scientific and Industrial Research (CSIR) funded network

project; HCP-0019 to PK, DST-INSPIRE-Senior Research Fellowship to AS, DBT-Senior Research Fellowship to SKA and UGC-Junior Research Fellowship to NS.

Conflicts of interest

The authors have declared that no competing interest exists regarding research, authorship, and publication of the article.

Acknowledgements

We are grateful to the Institutional Manuscript Review Committee of CSIR-IITR for approval and allocation of communication number 3614 for the manuscript. We are thankful to Mr Jai Shankar for his support in TEM instrumentation and to Dr Mahadeo Kumar for his support in performing biochemical analysis. We are also grateful to Dr Anjaneya Ayur, Scientist, CSIR-IITR and Mr Pankaj Jagdale for their support in carrying out histopathological studies.

References

1 E. M. Brunt, Pathology of nonalcoholic fatty liver disease, *Nat. Rev. Gastroenterol. Hepatol.*, 2010, **7**, 195e203.
2 B. W. A. Smith and L. A. Adams, Non-alcoholic fatty liver disease, *Crit. Rev. Clin. Lab. Sci.*, 2011, **48**, 97–113.
3 M. Krawczyk, L. Bonfrate and P. Portincasa, Nonalcoholic fatty liver disease, *Best Pract. Res., Clin. Gastroenterol.*, 2010, **24**, 695e708.
4 E. Buzzetti, M. Pinzani and E. A. Tsochatzis, The multiple-hit pathogenesis of non-alcoholic fatty liver disease (NAFLD), *Metabolism*, 2016, **65**, 1038–1048.
5 J. K. Dowman, J. W. Tomlinson and P. N. Newsome, Pathogenesis of nonalcoholic fatty liver disease, *QJM*, 2010, **103**, 71e83.
6 Q. Wang, S. Liu, A. Zhai, B. Zhang and G. Tian, AMPK-mediated regulation of lipid metabolism by phosphorylation, *Biol. Pharm. Bull.*, 2018, b17-00724.
7 S. Herzig and R. J. Shaw, AMPK: guardian of metabolism and mitochondrial homeostasis, *Nat. Rev. Mol. Cell Biol.*, 2018, **19**, 121.
8 J. T. Rodgers, C. Lerin, Z. Gerhart-Hines and P. Puigserver, Metabolic adaptations through the PGC–1α and SIRT1 pathways, *FEBS Lett.*, 2008, **582**, 46–53.
9 X. Ye, M. Li, T. Hou, T. Gao, W.-g. Zhu and Y. Yang, Sirtuins in glucose and lipid metabolism, *Oncotarget*, 2017, **8**, 1845.
10 A. Coste, J. F. Louet, M. Lagouge, C. Lerin, M. C. Antal, H. Meziane, K. Schoonjans, P. Puigserver, B. W. O'Malley and J. Auwerx, The genetic ablation of SRC-3 protects against obesity and improves insulin sensitivity by reducing the acetylation of PGC-1α, *Proc. Natl. Acad. Sci. U. S. A.*, 2008, **105**(44), 17187–17192.
11 X. Q. Deng, L. L. Chen and N. X. Li, The expression of SIRT1 in nonalcoholic fatty liver disease induced by high-fat diet in rats, *Liver Int.*, 2007, **27**(5), 708–715.
12 Y. Yang, W. Li, Y. Liu, Y. Sun, Y. Li, Q. Yao, J. Li, Q. Zhang, Y. Gao and L. Gao, Alpha-lipoic acid improves high-fat diet-induced hepatic steatosis by modulating the transcription factors SREBP-1, FoxO1 and Nrf2 via the SIRT1/LKB1/AMPK pathway, *J. Nutr. Biochem.*, 2014, **25**, 1207–1217.
13 T. F. Osborne, Sterol regulatory element-binding proteins (SREBPs): key regulators of nutritional homeostasis and insulin action, *J. Biol. Chem.*, 2000, **275**, 32379–32382.
14 Y. Li, S. Xu, M. M. Mihaylova, B. Zheng, X. Hou, B. Jiang, O. Park, Z. Luo, E. Lefai and J. Y. J. Shyy, AMPK phosphorylates and inhibits SREBP activity to attenuate hepatic steatosis and atherosclerosis in diet-induced insulin-resistant mice, *Cell Metab.*, 2011, **13**, 376–388.
15 Y.-A. Moon, G. Liang, X. Xie, M. Frank-Kamenetsky, K. Fitzgerald, V. Koteliansky, M. S. Brown, J. L. Goldstein and J. D. Horton, The Scap/SREBP pathway is essential for developing diabetic fatty liver and carbohydrate-induced hypertriglyceridemia in animals, *Cell Metab.*, 2012, **15**, 240–246.
16 J. Ye and R. A. DeBose-Boyd, Regulation of cholesterol and fatty acid synthesis, *Cold Spring Harbor Perspect. Biol.*, 2011, **3**, a004754.
17 M. P. Sajan, M. C. Lee, F. Foufelle, J. Sajan, C. Cleland and R. V. Farese, Coordinated regulation of hepatic FoxO1, PGC-1α and SREBP-1c facilitates insulin action and resistance, *Cell. Signalling*, 2018, **43**, 62–70.
18 S. Saha, D. P. Panigrahi, S. Patil and S. K. Bhutia, Autophagy in health and disease: A comprehensive review, *Biomed. Pharmacother.*, 2018, **104**, 485–495.
19 E. Morselli, M. C. Maiuri, M. Markaki, E. Megalou, A. Pasparaki, K. Palikaras, A. Criollo, L. Galluzzi, S. A. Malik, I. Vitale, M. Michaud, F. Madeo, N. Tavernarakis and G. Kroemer, Caloric restriction and resveratrol promote longevity through the Sirtuin-1-dependent induction of autophagy, *Cell Death Dis.*, 2010, **1**, e10.
20 C. J. Chang, T.-F. Tzeng, S.-S. Liou, Y.-S. Chang and I. M. Liu, Regulation of lipid disorders by ethanol extracts from Zingiber zerumbet in high-fat diet-induced rats, *Food Chem.*, 2012, **132**, 460–467.
21 P. L. Schiff Jr., Bisbenzylisoquinoline alkaloids, *J. Nat. Prod.*, 1991, **54**, 645–749.
22 C. Q. Xu, D. L. Dong, Z. M. Du, Q. W. Chen, D. M. Gong and B. F. Yang, Comparison of the anti-arrhythmic effects of matrine and berbamine with amiodarone and RP58866, *Acta Pharm. Sin.*, 2004, **39**, 691–694.
23 F. Yang, S. Nam, C. E. Brown, R. Zhao, R. Starr, D. A. Horne, L. H. Malkas, R. Jove and R. J. Hickey, A novel berbamine derivative inhibits cell viability and induces apoptosis in cancer stem-like cells of human glioblastoma, via up-regulation of miRNA-4284 and JNK/AP-1 signaling, *PLoS One*, 2014, **9**, e94443.
24 Y. Gu, T. Chen, Z. Meng, Y. Gan, X. Xu, G. Lou, H. Li, X. Gan, H. Zhou, J. Tang and G. Xu, CaMKII γ, a critical

regulator of CML stem/progenitor cells, is a target of the natural product berbamine, *Blood*, 2012, **120**(24), 4829–4839.
25 Y. Zhao, Y. Tan, G. Wu, L. Liu, Y. Wang, Y. Luo, J. Shi and H. Huang, Berbamine overcomes imatinib-induced neutropenia and permits cytogenetic responses in Chinese patients with chronic-phase chronic myeloid leukemia, *Int. J. Hematol.*, 2011, **94**, 156–162.
26 S. Wang, Q. Liu, Y. Zhang, K. Liu, P. Yu, J. Luan, H. Duan, Z. Lu, F. Wang, E. Wu, K. Yagasaki and G. Zhang, Suppression of growth, migration and invasion of highly-metastatic human breast cancer cells by berbamine and its molecular mechanisms of action, *Mol. Cancer*, 2009, **8**, 81.
27 S. Nam, J. Xie, A. Perkins, Y. Ma, F. Yang, J. Wu, Y. Wang, R.-z. Xu, W. Huang and D. A. Horne, Novel synthetic derivatives of the natural product berbamine inhibit Jak2/Stat3 signaling and induce apoptosis of human melanoma cells, *Mol. Oncol.*, 2012, **6**, 484–493.
28 A. Sharma, S. K. Anand, N. Singh, U. N. Dwivedi and P. Kakkar, Berbamine induced AMPK activation regulates mTOR/SREBP-1c axis and Nrf2/ARE pathway to allay lipid accumulation and oxidative stress in steatotic HepG2 cells, *Eur. J. Pharmacol.*, 2020, 173244.
29 C. Sankaranarayanan, R. Nishanthi and P. Pugalendi, Ameliorating effect of berbamine on hepatic key enzymes of carbohydrate metabolism in high-fat diet and streptozotocin induced type 2 diabetic rats, *Biomed. Pharmacother.*, 2018, **103**, 539–545.
30 M. R. Jain, S. R. Giri, B. Bhoi, C. Trivedi, A. Rath, R. Rathod, R. Ranvir, S. Kadam, H. Patel and P. Swain, Dual PPAR α/γ agonist Saroglitazar improves liver histopathology and biochemistry in experimental NASH models, *Liver Int.*, 2018, **38**, 1084–1094.
31 L. Shi, L. Shi, H. Zhang, Z. Hu, C. Wang, D. Zhang and G. Song, Oxymatrine ameliorates non-alcoholic fatty liver disease in rats through peroxisome proliferator-activated receptor-alpha activation, *Mol. Med. Rep.*, 2013, **8**, 439–445.
32 J. Folch, M. Lees and G. H. Sloane Stanley, A simple method for the isolation and purification of total lipids from animal tissues, *J. Biol. Chem.*, 1957, **226**, 497–509.
33 B. Wallin, B. Rosengren, H. G. Shertzer and G. Camejo, Lipoprotein oxidation and measurement of thiobarbituric acid reacting substances formation in a single microtiter plate: its use for evaluation of antioxidants, *Anal. Biochem.*, 1993, **208**, 10–15.
34 P. Kakkar, B. Das and P. N. Viswanathan, A modified spectrophotometric assay of superoxide dismutase, *Indian J. Biochem. Biophys.*, 1984, **21**, 130–132.
35 P. K. Smith, R. I. Krohn, G. T. Hermanson, A. K. Mallia, F. H. Gartner, M. D. Provenzano, E. K. Fujimoto, N. M. Goeke, B. J. Olson and D. C. Klenk, Measurement of protein using bicinchoninic acid, *Anal. Biochem.*, 1985, **150**, 76–85.
36 C. N. Perry, S. Kyoi, N. Hariharan, H. Takagi, J. Sadoshima and R. A. Gottlieb, Novel methods for measuring cardiac autophagy in vivo, *Methods Enzymol.*, 2009, **453**, 325–342.
37 D. O. Saleh, R. F. Ahmed and M. M. Amin, Modulatory role of Co-enzyme Q10 on methionine and choline deficient diet-induced non-alcoholic steatohepatitis (NASH) in albino rats, *Appl. Physiol., Nutr., Metab.*, 2016, **42**, 243–249.
38 I. Mikolasevic, V. Lukenda, S. Racki, S. Milic, B. Sladoje-Martinovic and L. Orlic, Nonalcoholic fatty liver disease (NAFLD)–a new factor that interplays between inflammation, malnutrition, and atherosclerosis in elderly hemodialysis patients, *Clin. Interventions Aging*, 2014, **9**, 1295.
39 M. Noureddin and R. Loomba, Nonalcoholic fatty liver disease: Indications for liver biopsy and noninvasive biomarkers, *Clin. Liver Dis.*, 2012, **1**, 104–107.
40 A. R. Saltiel and C. R. Kahn, Insulin signalling and the regulation of glucose and lipid metabolism, *Nature*, 2001, **414**, 799–806.
41 F. Bessone, M. V. Razori and M. G. Roma, Molecular pathways of nonalcoholic fatty liver disease development and progression, *Cell. Mol. Life Sci.*, 2019, **76**, 99–128.
42 A. Ayala, M. F. Munoz and S. Arguelles, Lipid peroxidation: production, metabolism, and signaling mechanisms of malondialdehyde and 4-hydroxy-2-nonenal, *Oxid. Med. Cell. Longevity*, 2014, **2014**, 360438.
43 J. D. Covington and S. Bajpeyi, The sirtuins: markers of metabolic health, *Mol. Nutr. Food Res.*, 2016, **60**, 79–91.
44 J. Li, M. Liu, H. Yu, W. Wang, L. Han, Q. Chen, J. Ruan, S. Wen, Y. Zhang and T. Wang, Mangiferin improves hepatic lipid metabolism mainly through its metabolite-norathyriol by modulating SIRT-1/AMPK/SREBP-1c signaling, *Front. Pharmacol.*, 2018, **9**, 201.
45 J. Kim, G. Yang, Y. Kim and J. Ha, AMPK activators: mechanisms of action and physiological activities, *Exp. Mol. Med.*, 2016, **48**, e224.
46 J. T. Nickels Jr., New links between lipid accumulation and cancer progression, *J. Biol. Chem.*, 2018, **293**, 6635–6636.
47 A. Montagner, A. Polizzi, E. Fouché, S. Ducheix, Y. Lippi, F. Lasserre, V. Barquissau, M. Régnier, C. Lukowicz and F. Benhamed, Liver PPARα is crucial for whole-body fatty acid homeostasis and is protective against NAFLD, *Gut*, 2016, **65**, 1202–1214.
48 J. Skat-Rørdam, D. Højland Ipsen, J. Lykkesfeldt and P. Tveden-Nyborg, A role of peroxisome proliferator–activated receptor γ in non–alcoholic fatty liver disease, *Basic Clin. Pharmacol. Toxicol.*, 2019, **124**, 528–537.
49 S. Ding, J. Jiang, G. Zhang, Y. Bu, G. Zhang and X. Zhao, Resveratrol and caloric restriction prevent hepatic steatosis by regulating SIRT1-autophagy pathway and alleviating endoplasmic reticulum stress in high-fat diet-fed rats, *PLoS One*, 2017, **12**, e0183541.
50 A. Stacchiotti, G. Favero, A. Lavazza, I. Golic, M. Aleksic, A. Korac, L. F. Rodella and R. Rezzani, Hepatic macrosteatosis is partially converted to microsteatosis by melatonin supplementation in ob/ob mice non-alcoholic fatty liver disease, *PLoS One*, 2016, **11**, e0148115.
51 C. Ding, Y. Zhao, X. Shi, N. Zhang, G. Zu, Z. Li, J. Zhou, D. Gao, L. Lv and X. Tian, New insights into salvianolic acid A action: Regulation of the TXNIP/NLRP3 and TXNIP/

ChREBP pathways ameliorates HFD-induced NAFLD in rats, *Sci. Rep.*, 2016, **6**, 28734.

52 J. Massart, K. Begriche, C. Moreau and B. Fromenty, Role of nonalcoholic fatty liver disease as risk factor for drug-induced hepatotoxicity, *J. Clin. Transl. Res.*, 2017, **3**, 212.

53 Z. Ma, L. Chu, H. Liu, W. Wang, J. Li, W. Yao, J. Yi and Y. Gao, Beneficial effects of paeoniflorin on non-alcoholic fatty liver disease induced by high-fat diet in rats, *Sci. Rep.*, 2017, **7**, 44819.

54 F. Haczeyni, M. M. Yeh, G. N. Ioannou, I. A. Leclercq, R. Goldin, Y. Y. Dan, J. Yu, N. C. Teoh and G. C. Farrell, Mouse models of non–alcoholic steatohepatitis: A reflection on recent literature, *J. Gastroenterol. Hepatol.*, 2018, **33**, 1312–1320.

55 H. Yao, Y.-J. Qiao, Y.-L. Zhao, X.-F. Tao, L.-N. Xu, L.-H. Yin, Y. Qi and J.-Y. Peng, Herbal medicines and nonalcoholic fatty liver disease, *World J. Gastroenterol.*, 2016, **22**, 6890.

56 L.-f. Li, Y. Guo, G.-t. Tang, X. Cao, C.-y. Yu and L.-x. Chen, Mechanism of hepatic insulin resistance induced by high-fat diet, *Chin. J. Pathophysiol.*, 2011, **27**, 310–314.

57 A. Gonzalez, C. Huerta-Salgado, J. Orozco-Aguilar, F. Aguirre, F. Tacchi, F. Simon and C. Cabello-Verrugio, Role of Oxidative Stress in Hepatic and Extrahepatic Dysfunctions during Nonalcoholic Fatty Liver Disease (NAFLD), *Oxid. Med. Cell. Longevity*, 2020, **2020**, DOI: 10.1155/2020/1617805.

58 D. Garcia and R. J. Shaw, AMPK: Mechanisms of Cellular Energy Sensing and Restoration of Metabolic Balance, *Mol. Cell*, 2017, **66**, 789–800.

59 A. Satoh, L. Stein and S. Imai, The role of mammalian sirtuins in the regulation of metabolism, aging, and longevity, *Handb. Exp. Pharmacol.*, 2011, **206**, 125–162.

60 F. Wang, X. Yang, Y. Lu, Z. Li, Y. Xu, J. Hu, J. Liu and W. Xiong, The natural product antroalbol H promotes phosphorylation of liver kinase B1 (LKB1) at threonine 189 and thereby enhances cellular glucose uptake, *J. Biol. Chem.*, 2019, **294**(27), 10415–10427.

61 Y. Zhang, C. Geng, X. Liu, M. Li, M. Gao, X. Liu, F. Fang and Y. Chang, Celastrol ameliorates liver metabolic damage caused by a high-fat diet through Sirt1, *Mol. Metab.*, 2017, **6**, 138–147.

62 W. Zhang, Q. Huang, Z. Zeng, J. Wu, Y. Zhang and Z. Chen, Sirt1 inhibits oxidative stress in vascular endothelial cells, *Oxid. Med. Cell. Longevity*, 2017, DOI: 10.1155/2017/7543973.

63 Y. Li, S. Xu, M. M. Mihaylova, B. Zheng, X. Hou, B. Jiang, O. Park, Z. Luo, E. Lefai and J. Y.-J. Shyy, AMPK phosphorylates and inhibits SREBP activity to attenuate hepatic steatosis and atherosclerosis in diet-induced insulin-resistant mice, *Cell Metab.*, 2011, **13**, 376–388.

64 H. Shimano and R. Sato, SREBP-regulated lipid metabolism: convergent physiology—divergent pathophysiology, *Nat. Rev. Endocrinol.*, 2017, **13**, 710.

65 W. Wahli and L. Michalik, PPARs at the crossroads of lipid signaling and inflammation, *Trends Endocrinol. Metab.*, 2012, **23**, 351–363.

66 D. G. Hardie, AMP-activated protein kinase—an energy sensor that regulates all aspects of cell function, *Genes Dev.*, 2011, **25**, 1895–1908.

67 A.-M. Lundsgaard, A. M. Fritzen and B. Kiens, Molecular regulation of fatty acid oxidation in skeletal muscle during aerobic exercise, *Trends Endocrinol. Metab.*, 2018, **29**, 18–30.

68 V. Lahiri, W. D. Hawkins and D. J. Klionsky, Watch what you (self-) eat: autophagic mechanisms that modulate metabolism, *Cell Metab.*, 2019, **29**, 803–826.

69 H. X. Yuan, Y. Xiong and K. L. Guan, Nutrient sensing, metabolism, and cell growth control, *Mol. cell.*, 2013, **49**(3), 379–387.

70 H. Dong and M. J. Czaja, Regulation of lipid droplets by autophagy, *Trends Endocrinol. Metab.*, 2011, **22**(6), 234–240.